Review of Materials Research 1 (2025) 100013

Contents lists available at ScienceDirect

Review of Materials Research

journal homepage: www.sciencedirect.com/journal/review-of-materials-research

Progress and perspectives on molecular design of crosslinked polymer electrolytes for solid-state lithium batteries

Fei Pei [a], Lin Wu [a], Wenjie Lin [a], Yi Zhang [a], Qi Kang [b], Fenghua Zhang [a], Yuan Shen [c], Qiang Gao [a], Zhenyu Huang [a], Yunhui Huang [a,*]

[a] State Key Laboratory of Materials Processing and Die & Mould Technology, School of Materials Science and Engineering, Huazhong University of Science and Technology, Wuhan, 430074, China
[b] Institute of New Energy for Vehicles, School of Materials Science and Engineering, Tongji University, Shanghai, 201804, China
[c] Zhejiang Geely Holding Group Co., Ltd., Hangzhou, 310051, China

ARTICLE INFO

Keywords:
Crosslinked polymer electrolytes
Solid-state lithium batteries
Physical crosslinking
Chemical crosslinking
High energy density

ABSTRACT

Solid-state polymer electrolytes (SPEs) coupling with high-specific-energy cathodes/anodes are candidate schemes for meeting the safety and energy density needs of next generation lithium batteries due to the reinforced mechanical/chemical and electrochemical stability. However, many pressing challenges, such as low ionic conductivity, large interfacial resistance and side reactions, hindering their practical applications in solid-state lithium batteries (SSLBs). Crosslinked SPEs as one of the most attractive structures exhibit many advantages, such as superior mechanical strength, thermal/chemical stability, and reduced crystallinity. The design/synthesis strategies of crosslinked SPEs and how do the geometric structural parameters affect electrochemical performance of the SPEs are not fully understood. This review comprehensively summarizes the very recent advances of crosslinked SPEs for SSLBs by discussing the related publications, which involves physical and chemical crosslinking strategies. The selection of crosslinked monomers and reaction type are classified in detail. The relationships between crosslinking structures and physical/electrochemical properties at molecular level are comprehensive analyzed. Finally, the challenges and future prospects of crosslinked SPEs in this rapidly evolving field are outlined. Overall, this review is expected to serve as a guide for designing high-performance crosslinked SPEs, and will receive widespread attention in the field of binders, separators, hydrogels, electronic skin and engineering plastics.

1. Introduction

Next-generation electric vehicles and large-scale energy storage are thriving in the global context of carbon neutrality, lithium-ion batteries (LIBs) have gained tremendous success as an energy-storage system. However, the escalating demand for higher energy density and safety can hardly satisfy the ever-increasing demand in portable electronics and electric vehicles, presents a formidable challenge for state-of-the-art LIBs based on intercalation chemistry and liquid electrolyte [1–4].

High-voltage cathode materials (such as high-nickel, Li-rich Mn-based layered oxide or sulfur) matched with lithium-metal (Li) or silicon-based (Si) anode materials have been identified as one of the most promising optimal choice beyond traditional LIBs due to the higher theoretical capacity and operating voltage [5–13]. The most concerned safety hazards come along with the increased energy density of LIBs, this severely limits the further development of many high specific energy battery systems. Up to now, the commercialized LIBs heavily depend on the utilization of organic liquid electrolytes (LE), which can lead to a series of severe safety problems, including oxidation/decomposition thermal runaway, burning or explosion [14,15]. This puts forward higher requirements for the safety of lithium-based batteries especially with the boom in electric vehicles. To address these issues, solid-state lithium-based batteries (SSLBs), by replacing LE with solid-state electrolytes, has been viewed as a safe choice and received much attention and research recently [16–18]. Solid-state polymer electrolytes (SPEs) can meet the safety and energy density needs of advanced SSLBs due to their improved mechanical property, excellent electrochemical stability, flexibility and processability.

The research of SPEs began with the exploration of the conductivity of poly(ethylene oxide) (PEO) and alkali metal ion complexes by Wright

* Corresponding author.
E-mail address: huangyh@hust.edu.cn (Y. Huang).

https://doi.org/10.1016/j.revmat.2025.100013
Received 21 March 2025; Received in revised form 6 April 2025; Accepted 6 April 2025
Available online 8 April 2025

et al., in 1973 [19]. Then Armand et al. in France reported that the Li^+ conductivity of PEO with alkali metal salt complex reached 10^{-5} S cm^{-1} at 40–60 °C in 1979, showing good film forming property, which could be used as electrolyte of LIBs [4]. The results show that the SPE formed by PEO and alkali metal salts has three phase regions at room temperature: amorphous phase, pure PEO phase and salt-rich phase, in which the Li^+ conduction occurs in the amorphous phase. The ion conductive mechanism of SPEs is generally believed to be: Lithium salts are complexed with polar functional groups on the polymer chain, which promotes the dissociation of lithium salt and the transport of Li^+ ions. Under the action of electric field, with the thermal movement of the polymer chain segments in the high elastic region, the Li^+ ions and the polar groups continue to complexation/de-complexation process, achieving the conduction of Li^+ ions.

However, the bottleneck of SPEs, such as the unsatisfied ionic conductivity at room temperature (such as the most common linear PEO, 10^{-7}~10^{-5} S cm^{-1}), relatively narrow electrochemical stability window with the cutoff voltage less than 4.0 V, large solid/solid interfacial resistance and non-ideal electrode/electrolyte compatibility, still restrict further commercialization of SPEs in SSLBs. This issue is even more pronounced in high-energy-density battery systems when coupling with high-voltage cathodes (such as $LiNi_{1-x-y}Co_xMn_yO_2$, $LiNi_{1-x-y}Co_xAl_yO_2$, $LiCoO_2$ or $xLi_2MnO_3{\cdot}(1\text{-}x)LiMO_2$) [20–23].

Over the last decades, crosslinked polymers as one of the most representative polymers, which deliver desirable mechanical properties, elasticity, and thermal/chemical stability, have been widely used in aerospace engineering, smart electronics, intelligent architecture, and other high-tech fields. Recently, with the assistance of huge technique progress on the polymerization synthesis strategy, characterization methods, and theoretical calculation, plenty of crosslinked SPEs have been developed into the field of SSLBs. Crosslinked polymers have been widely used in many applications, particularly for hydrogels, fuel cells, electronic skin, and engineering plastics. Owing to the strong mechanical strength, physicochemical stability and excellent ionic conductivity of the recently reported crosslinked SPEs, constructing crosslinked SPEs appears to be a more appropriate strategy to promote the electrochemical performance of SSLBs. Crosslinked SPEs are highlighted because of: (i) Three-dimensional crosslinked polymer networks can significantly improve the mechanical strength and elasticity of polymers, effectively inhibiting the short circuit caused by Li dendrites and the stress/strain caused by the volume expansion of electrode materials; (ii) The interaction between molecular chains in crosslinked polymers can give the polymers novel properties, such as dynamic self-healing and shape memory, which help to understand the relationships between structure and physical property at molecular level; (iii) Compared with the linear chain polymer molecules, the crosslinked structure helps to break the ordered arrangement of the polymer chain and reduce the polymer crystallinity, improving the thermal motion of the molecular chain and efficient Li^+ ion transport. Based on the above advantages, crosslinked polymer electrolytes have begun to attract great attention from researchers.

In this review, we briefly review the strategies of molecular structure design and regulation of crosslinked SPEs at the molecular level for long-life and high-energy-density SSLBs, which are include physical crosslinking and chemical crosslinking strategies (Fig. 1). First, we start by introducing the fundamentals of solid-state polymer electrolytes, as well

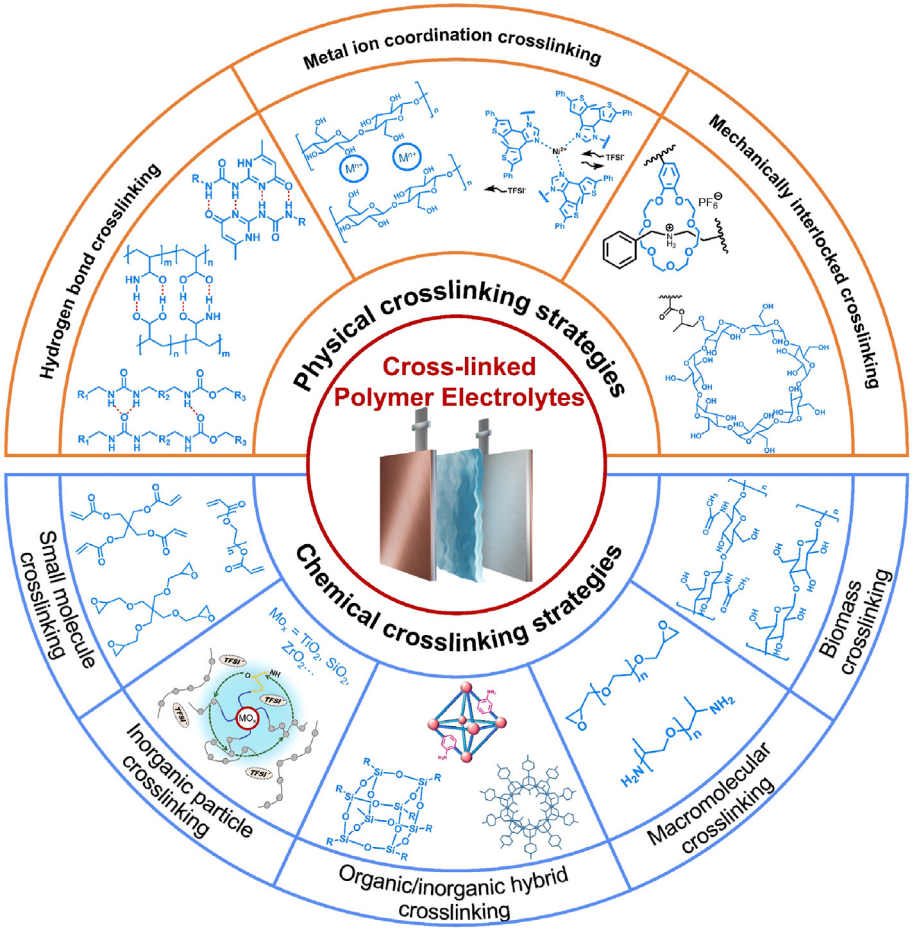

Fig. 1. The hierarchical schematic of universal design strategies for crosslinked polymer electrolytes, including physical crosslinking and chemical crosslinking strategies.

as their key challenges and potential solutions. Next, both physical and chemical crosslinking strategies are classified in detail, the selection of crosslinked monomers and reaction type of crosslinked SPEs are classified in detail. The relationships between crosslinking structure and physical/electrochemical properties at molecular level are comprehensive analyzed. Finally, the optimization and in-situ characterization of the intrinsic properties of crosslinked SPEs are summarized and prospected. We believe that this review will contribute to guiding the molecular design of SPEs and industrial application of high-performance SSLBs in the future.

2. Fundamentals and challenges

According to the types of polymerization reaction and the choice of monomers, a series of SPEs with different structure types have been designed and synthesized. In addition to the common straight-chain polymers, such as poly(ethylene oxide) (PEO), polyvinylidene difluoride (PVDF), polyacrylonitrile (PAN) and polymethyl methacrylate (PMMA), etc. [23–25] Some SPEs with special structures have been gradually discovered, such as single-ion conductor polymers, block copolymers, star structures, hyperbranched structures, bottlebrush-like and crosslinked structures, etc. These unique structures have improved the electrochemical properties of SPEs to various degrees. The conduction mechanism of Li^+ ions in polymers has been deeply studied, such as polar functional groups, crystallization region, glass transition temperature (T_g) and other influencing factors. However, the classification of mechanism design strategies, the effects of structural parameters on physicochemical properties and electrochemical properties of SPEs are rarely summarized. The key challenges that hinder the practical application of SPEs include.

2.1. Ionic conductivity

Among all disadvantages that SPEs suffer, the unsatisfactory ionic conductivity of SPEs than that of liquid electrolytes (LE) manifests a serious barrier to high electrochemical performance. The lithium salts are dissolved in the polymers and migrate by the thermal motion of the polymer chain segments. According to the universally accepted Li^+ transport model in SPEs, Li^+ ions are coupled with the thermal motion of the polymer chain segments, Li^+ can transport or hop to adjacent coordinated sites through various polar functional groups on the macromolecular chains, such as carbonyl (−C=O), ether (C−O−C), nitrile (−C ≡ N), and fluoride (C−F) (for example, polycarbonates (PC), polyether (PE), polyacrylonitrile (PAN) and polyvinylidene difluoride (PVDF)) [26]. Besides, ionic conductivity of the SPEs is generally controlled by the Vogel-Tamman-Fulcher (VTF) model, indicating that low glass transition temperatures (T_g) value leads to high speed lithium ion migration and ionic conductivity in SPEs.

2.2. Electrochemical stability

The common strategies for evaluating electrochemical stability of SPEs are measured by the linear scan voltammograms (LSV) or electrochemical floating analysis. The stabilities of SPEs directly determine their compatibility with high-voltage cathodes and Li-metal anodes. Besides, theoretical calculations and simulation have been applied to study the electrochemical stability window of SPEs by evaluating the highest occupied molecular orbital (HOMO) and lowest unoccupied molecular orbital (LUMO) energy level of the monomers, polymers, lithium salts or additives [27]. It is well known that the PEO-based SPEs are slowly oxidized at voltages >3.8 V, restricting its further application in high-energy-density SSLBs. Thus, the polymer matrix and Li salts can be rationally designed to further broaden the electrochemical stability windows.

2.3. Glass transition temperature and crystallinity

As one of the pivotal influencing factors of amorphous polymer materials, glass transition directly affects the ion transport properties of SPEs. Above the glass transition temperature (T_g), the polymer chain segment begins to thermal motion, showing a high elastic property. Along with the temperature continue to rise, the polymer chain will move and show a viscous flow property. Generally, T_g can be tested by differential scanning calorimetry (DSC). The molecular structure, geometry, and molecular weight have a direct influence on T_g. Reducing the T_g can significantly enhance the segmental mobility of the polymer chains at a higher temperature. Above T_g, with the thermal motion of the polymer chain segments, the Li^+ ion can migrate from one coordination site to the next site along the molecular chains. Alternatively, the Li^+ ion can hop from one chain to another under the effect of an electric field. Reducing the T_g is one of the most efficient strategies to improve the Li^+ conductivity [24].

The molecular structure of polymers with good symmetry, without branch chain or small side group volume, and large intermolecular forces are easy to be close to each other, and the tightly ordered regions are easy to crystallization. High crystallinity usually means that the movement of the molecular chain is limited because the molecular chains are locked in a fixed position within the crystalline region. In contrast, in the amorphous region, the molecular chains can move more freely. Amorphous can act as channels for ion transport because they provide a path of lower resistance that allows ions to pass through.

2.4. Mechanical strength

The mechanical properties of the SPEs directly determine the core safety issues of the battery. Such as Young's modulus, elasticity, and self-healing properties, which can be a good solution to the stress-strain problems of the next generation of high specific energy electrode materials such as high nickel oxide, sulfur, silicon, and Li metal (severe volume expansion during cycling) [10,28]. (i) The excellent elastic structure of SPEs can inhibit the volume expansion/contraction of the active materials during cycling process; (ii) The high Young's modulus can inhibit the safety hazards such as the short circuit caused by the Li dendrites piercing the electrolyte; (iii) The self-healing property can automatically repair the cracking of the electrodes during cycling. However, the mechanical strength of SPEs will show a significant decline after adding a large amount of lithium salts and plasticizers. Especially at present, in order to improve the energy density, the continuous pursuit of ultra-thin SPEs structure puts higher requirements on the mechanical strength of the SPEs.

2.5. Solid-solid interface contact

The fabrication SSLBs involve multiple steps including the preparation of self-supporting SPEs films and laminated assembly process. The physical contact resistance is caused by poor solid-solid contact at the electrode/electrolyte interfaces, which results in poor electrode/electrolyte interface contact/compatibility and unsatisfactory electrochemical performance compared with LE [29,30]. In addition to this, during cycling, even feeble stress-strain at the rigid solid-solid interfaces could lead to electrochemical failures. These failures include crack formation or delamination between the electrodes and SPEs, which significantly increase the interfacial resistance, reduce the cycling performance and even lead to performance failure.

Molecular architectural engineering of crosslinked SPEs can achieve a remarkable Li^+ conductivity without sacrificing mechanical/chemical strength and electrochemical properties of SPEs. Therefore, this brings us to the following interesting questions. (i) What are the advantages and special properties of crosslinked polymers compared to traditional straight chain polymers? (ii) What are the detailed classifications of the molecular structure of crosslinked SPEs? (iii) How to select the

monomers and reaction types of crosslinked polymer electrolytes rationally? (iv) What is the mechanism of performance improvement behind this atomic-level structural design? In this review, we comprehensively summarize the recent publication of crosslinked SPEs in addressing the key challenges in the next section by stating and discussing their crosslinking type and underlying mechanisms.

3. Physical crosslinking

Physical crosslinking refers to the interaction of two or more polymer molecules through a single physical interaction, such as electrostatic interaction, hydrogen bonding, ion coordination or chain entanglement/interpenetration (mechanical interlock). The structure of composite crosslinked polymer is formed without affecting the original molecular structures. In the structural design methods of SPEs, physical crosslinking is one of the most common strategies to improve the mechanical strength and electrochemical performance of SPEs. In this section, we focus on hydrogen bond (H-bonds) crosslinking, metal ion coordination crosslinking, and mechanical interlocked crosslinking strategies in detail.

3.1. H-bonds and multiple H-bonds crosslinking

The high energy density solid-state energy storage devices inevitably suffer from mechanical failure, bend/twist, and cracks during their long service life, which lead to serious security risks. Therefore, it is desirable to fabricate intelligent polymers that can restore original functionalities after physical/chemical damage to satisfy practical application requirements in various emerging fields [31,32]. At the intersection between chemistry and physics, there exists a special intermolecular force: hydrogen bonds. This hydrogen bond force in polymer science can achieve physical crosslinking, this is the so-called "hydrogen bond physical crosslinking". This physical crosslinked network can be reversibly formed

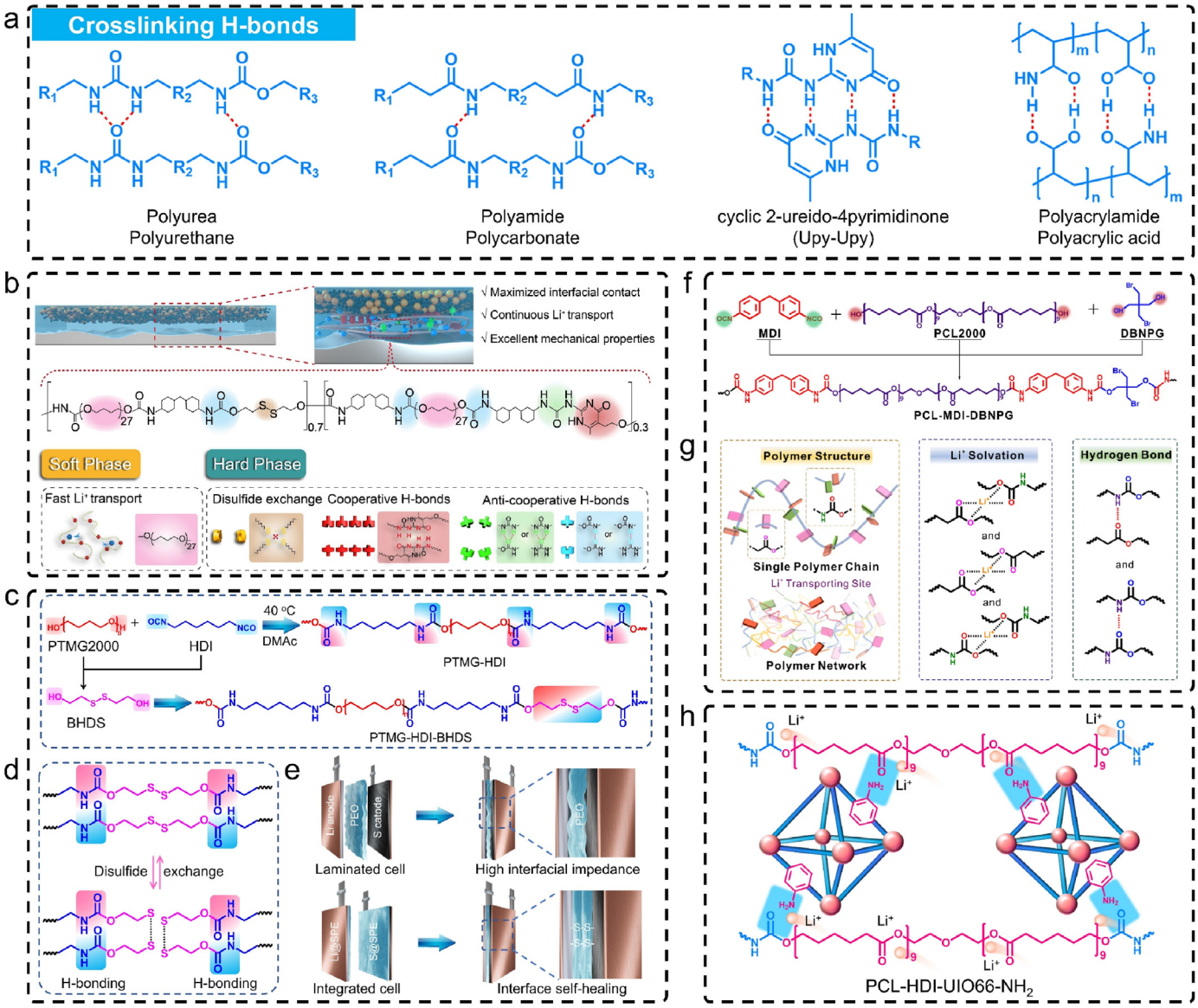

Fig. 2. Hydrogen bond crosslinking strategy applied to design polymer electrolytes. a) Schematic diagram of various hydrogen bond structures in the field of SPEs. b) Dynamic supramolecular polymer electrolyte network with multiple dynamic bonds including disulfide bonds (S–S) and multiple H-bonds (UPy-UPy) [30]. Copyright 2023, Wiley-VCH. c) Chemical structures of PTMG-HDI and PTMG-HDI-BHDS. d) The dynamic covalent self-healing disulfide bonds and H-bonds. e) Structure comparison of the conventional laminated and the integrated electrode/electrolyte solid-state batteries [29]. Copyright 2024, Nature Publish Group. f) Schematic illustration of PCL-MDI-DBNPG structure. g) Coordination effect of Li^+ with O and hydrogen bond formed between NH− and COO− [42]. Copyright 2021, Wiley-VCH. h) Schematic diagram of H-bonds between PCL-HDI and UIO-66-NH_2 [43]. Copyright 2024, Springer Heidelberg.

and dissociated under certain conditions, thus giving the polymer unique properties, such as high elasticity, self-healing and shape memory effect, etc. [33–35] H-bonds are widely used in various fields of batteries, such as binders, functional separators, electrolytes and electrode materials. Especially, H-bonds in SPEs play a crucial role to improve mechanical strength and dynamic self-healing properties.

Hydrogen atoms can form H-bonds with highly electronegative atoms (e.g., N, O, F). H-bonds in polymers occur mainly between functional groups containing hydroxyl (−OH), amino ($-NH_2$), carbonyl (C=O), and carboxylic (−COOH) groups (Fig. 2a) [36–39]. As one of the most common SPEs, poly(ether-urethane) is usually formed by stepwise polymerization of polyalcohols (e.g., polyether (PEG), polytetrahydrofuran (PTMG), or polycaprolactone (PCL)) and polyisocyanates, H-bond networks are formed between the repeated urethane groups (−NH−COO−) in the main framework. Therefore, poly(ether-urethane) is widely used in the field of SPEs [40,41]. Due to the limited solid-solid physical contact of the electrolyte-electrode interfaces, Ding et al. constructed an integrated cathode/SPE for SSLMBs by designing crosslinked dynamic supramolecular ionic conductive elastomers (DSICE) molecular structure (Fig. 2b) [30]. Multiple dynamic bonds, such as disulfide bonds (S−S), borate ester bonds, strong multiple H-bonds (UPy-UPy) and weak H-bonds (urethane-urethane or urea-urethane) were introduced into the polyurethane framework to enhance mechanical properties and the self-rapairing structure. The DSICE concurrently was utilized as $LiFePO_4$ (LFP) binders and SPE, providing consecutive Li^+ transport and uniform Li^+ deposition, such well-constructed Li|DSICE|LFP cells with the SPE thickness of 12 μm further delivered superior long-term cycling stability (> 600 cycles) and high capacity retention (80 % after 400 cycles). To solve the interface problem in SSLMBs, compared with traditional laminated assembly method with high interfacial resistance. Huang et al. designed a novel poly(ether-urethane)-based SPEs (PTMG-HDI-BHDS) for high-energy density SSLMBs, which was used to resolve the solid-solid interface contact of electrodes/SPEs (Fig. 2c) [29]. The hydroxyls (−OH) of polytetrahydrofuran (PTMG) reacted readily with hexamethylene diisocyanate (HDI). The chain extender of 2-hydroxyethyl disulfide (BHDS) was introduced to form poly(ether-urethane) (PTMG-HDI-BHDS) with self-healing character. The dynamic covalent disulfide bonds (S−S) and H-bonds provide excellent interfacial self-healing ability to repair ulti-interface problems (30 °C for 1 h) (Fig. 2d and e). As a result, the mechanical properties of PTMG-HDI-BHDS were 88.3 MPa (breaking strength) and 2000 % (ultimate elongation). The sulfurized polyacrylonitrile (SPAN) cathode delivered a significantly improved cycling stability (93 % capacity retention after 700 cycles) and rate performance (560 mAh g^{-1}_{SPAN} at 1C). Recently, they also report a nonflammable polyurethane electrolyte (PCL-MDI-DBNPG) by introducing flame retardant molecules (2,2-bis(bromomethyl)-1,3-propanediol (DBNPG)) in the form of covalent bonds (Fig. 2f) [42]. The abundant C=O and C−O−C functional groups in the polycaprolactone diol (PCL) soft segment can act as Li^+ complexation sites to promote the dissociation of lithium bis(trifluoromethanesulfonyl)imide salt (LiTFSI) (Fig. 2g). The repeated −NH−COO− and −COO− groups introduce abundant H-bonds network to endow SPEs with self-healing properties. The molecular weight of PCL-MDI-DBNPG improved by the chain extender of DBNPG significantly improved mechanical strength with a tensile elongation up to 1400 %. A low activation energy (0.35 eV), wide electrochemical window (5.1 V) was obtained. Pei et al. proposed $-NH_2$ modified metal-organic frameworks (UiO-66-NH_2) as multifunctional nano-fillers in the PU-based SPEs (PCL-HDI), achieving the collaborative promotion of the mechanical strength (42.8 MPa) and room temperature ionic conductivity (2.1×10^{-4} S cm^{-1}) (Fig. 2h) [43]. The surface modified $-NH_2$ groups and repeated −NH−COO− and −COO− groups can form H-bond network on polycarbonate-based PU frameworks. The interfaces between UiO-66-NH_2 and PU significantly decrease the crystallization of PCL-HDI and improve ion transport efficiency. As a result, $LiFePO_4$|SPEs|Li cells exhibit excellent cyclability for 700 cycles at 0.5C with a high capacity retention of ~97 %.

In general, the strength of a single H-bond is relatively weak, with a bond energy (~5 − 30 kJ mol^{-1}) of about one-tenth that of covalent bonds (~345 kJ mol^{-1} for C−C bonds). Efforts have been made to improve multiple H-bonds interaction. Double, triple, quadruple, sextuple and octuple H-bonds have been successively developed [36,44,45]. Alternatively, the multiple H-bonds (such as 2-ureido-4-pyrimidone (UPy)) can provide a stronger crosslinked skeleton with dynamic self-healing character [46]. To avoid the trade-off effect between Li^+ conductivity and mechanical strength in SPEs, Cui et al. Proposed a supramolecular Li^+ conductor in which the strong quadruple hydrogen-bonding UPy is included in the backbone to enhance the mechanical strength [38]. The strong association constant between UPy repetitive unit makes the H-bonds as strong as covalent bonds due to the reversible nature and dynamic properties, creating an enhanced breaking strength (~29 MJ m^{-3}) and high Li^+ conductivity (1.2×10^{-4} S cm^{-1} at 25 °C). Therefore, more types of multiple H-bonds have wider application prospects in the field of crosslinked polymer electrolytes.

However, significant variability among reported strategies (e.g., molecular weight, hydrogen bond types (e.g., F, N, O or S), density, steric effects, and hydrogen bond concentration) has led to irregular trends in physicochemical properties of SPEs. These inconsistencies likely arise from uncontrolled variables in polymer molecular structures across studies. This is the main reason why the H-bonded physical cross-linking strategy requires further in-depth research.

3.2. Metal ion coordination crosslinking

Metal coordination is one of the most common methods used for the construction of crosslinked polymers that are used in biomedical, environmental governance, electrochemical energy storage and other fields. Usually, metal ions (e.g., Ca^{2+}, Cu^{2+}, Fe^{3+}, Co^{2+}) with positive charge will form a coordination covalent bond structure with anions or negatively charged functional groups in polymer molecules when their electronic shell is not full, and eventually form a stable physical coordination crosslinked complex, which significantly improves mechanical strength, thermal stability and ion transport, making it an attractive method for crosslinking [47–50].

The polymers with multiple coordination functional groups are often used as the basic materials for coordination crosslinking. Hu et al. report a generalduty method for achieving high-performance Li^+ conductors by engineering of molecular channels (Fig. 3a) [51]. Through the coordination of copper ions (Cu^{2+}) with one-dimensional (1D) cellulose nanofibers which are rich in oxygen-containing polar functional groups (for example, hydroxyl), the opening of macromolecular chain within the normally ion-insulating cellulose enables rapid transport of Li^+ along the cellulose chains. As a result, the Cu^{2+}-coordinated cellulose SPE shows high Li^+ conductivity (1.5×10^{-3} S cm^{-1} at room temperature), high transference number (0.78) and a wide window of electrochemical stability (4.5 V) that can match both the high-voltage cathodes and Li anode. This 1D ion conductor also act as an effective ion-conducting binder of cathode, allowing ion transport in thick $LiFePO_4$ cathodes for high energy density SSLIMBs. Similarly, in the field of binders, ionic coordination crosslinking is also widely used. Zheng et al. constructed a 3D crosslinked polymer network as an enhanced binder for high-performance silicon anodes through coordination alginate chains with Ca^{2+} cations (Fig. 3b) [52]. The highly crosslinked alginate network exhibited enhanced mechanical strength and strongly interacted on Si particles, tolerating the severe volume expansion of Si anode to a large degree.

Some metal fluoride functional additives (M_xF_y) can not only form ionic coordination crosslinked structures with SPEs, but also participate in forming more stable solid electrolyte interphase (SEI). Huang et al. introduce a low content of CuF_2 (<0.5 wt%) into PEO-based SPE to improve the Li^+ conductivity through the strong coordination crosslinking effect between Cu^{2+} and O atoms from PEO/LiTFSI matrix [56].

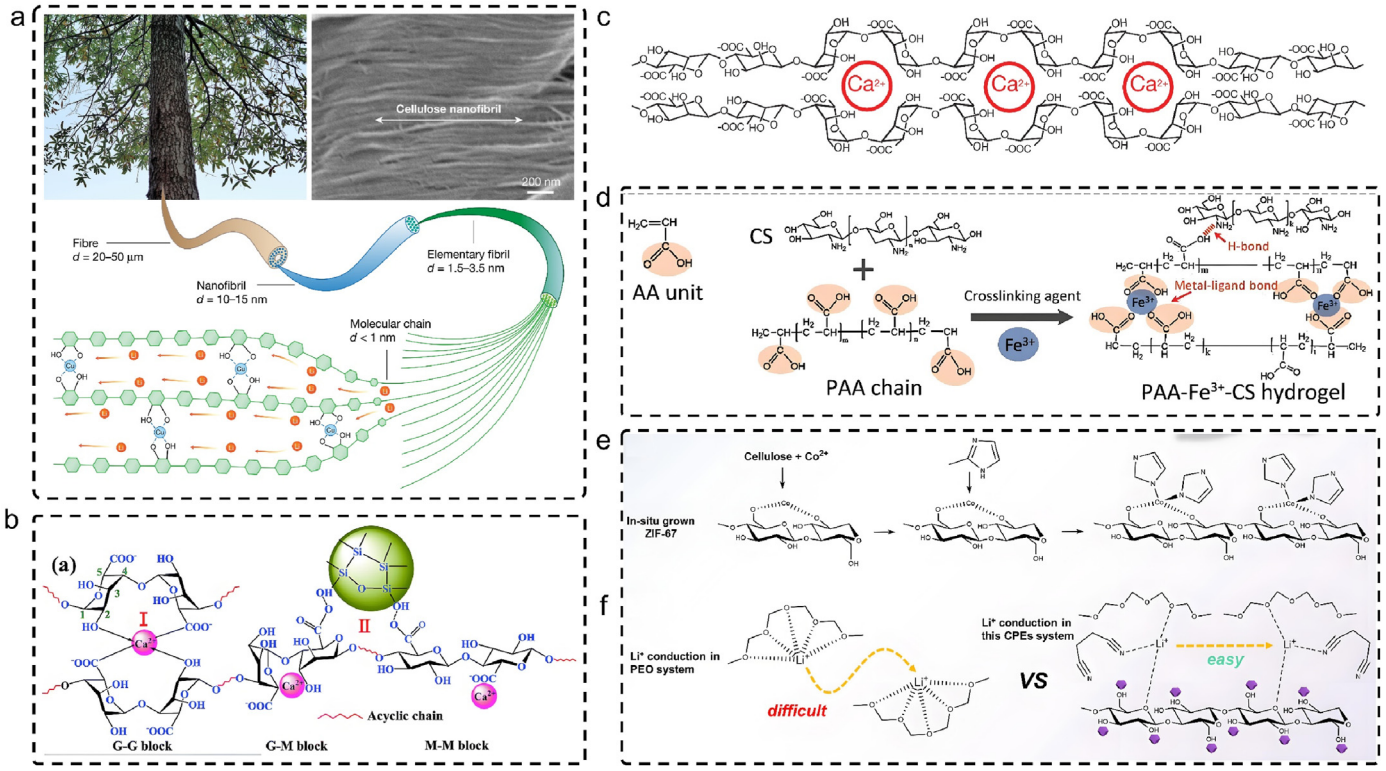

Fig. 3. Polymer electrolytes crosslinked by metal ion coordination. a) Coordination of Cu^{2+} ions with the −OH of cellulose fibres opens the spacing between the molecular chains, creating Li^+-conducting pathways [51]. Copyright 2021, Nature Publish Group. **b)** Chemical structure of sodium alginate and its network formation in the presence of calcium chloride [52]. Copyright 2014, The Royal Society of Chemistry. **c)** Molecular structure of ionic crosslinks between alginate chains and Ca^{2+} [53]. Copyright 2012, Nature Publish Group. **d)** Schematic depiction of the mechanism of PAA-Fe^{3+}-CS gel [54]. Copyright 2022, Wiley-VCH. **e, f)** In-situ grown process of ZIF-67 on cellulose fiber (CF) through Co^{2+} (e) and Li^+ conduction mechanism in SPEs after adding ZIF-67@CF and SN to the PEO matrix (f) [55]. Copyright 2024, Nature Publish Group.

The obtained PEO-CuF_2-LiTFSI SPE achieved an impressive Li^+ conductivity of 0.2 mS cm^{-1} (30 °C). Furthermore, the LiF-rich SEI was formed by CuF_2, enabling uniform Li^+ deposition during plating/stripping. As a result, the Li|SPE|$LiNi_{0.83}Co_{0.12}Mn_{0.05}O_2$ (NCM83) cell with PEO-Cu-F_2-LiTFSI exhibits a long cycling life over 500 cycles with 71 % capacity retention.

As a kind of semi-solid-state electrolytes between the liquid electrolytes (LE) and SPEs, the gel polymer electrolyte (GPEs) combines the advantages of both while allowing Li^+ ions to be transported in the swelling gel phase or liquid phase. The GPEs consists of polymer matrix, electrolyte salt and plasticizer, and usually exhibits unsatisfactory mechanical behaviour due to the large amount of LE stored in the polymer network. Suo et al. designed an extremely stretchable and tough gel by reacting two types of crosslinkers: ionically crosslinked alginate with $CaSO_4$, and covalently crosslinked polyacrylamide (Fig. 3c) [53]. They can be stretched beyond 20 times of original length with breaking strength of 9000 J m^{-2}. The excellent mechanical propertiesof gel is attributed to the synergistic effect of two mechanisms: crack bridging by the network of covalent crosslinks, and hysteresis by unzipping the network of Ca^{2+} crosslinks. Tan et al. introduced sodium alginate (SA) and calcium ions (Ca^{2+}) into PEO by ionic cross-linking to improve the mechanical properties of SPE [50]. The cross-linking process ensured the structure stability and flame-retardant performance, enhancing the mechanical strength and thermal stability of the solid-state batteries, so that it can maintain the integrity of morphology even at 120 °C, avoid short circuit caused by cathodes/anodes contact, and greatly improve the safety of LFP-based SSLMBs (2C for 100 cycles).

Furthermore, Hu et al. developed a GPE by using dual-network crosslinked polyacrylic acid-Fe^{3+}-chitosan (PAA-Fe^{3+}-CS) (Fig. 3d) [54]. The interconnected framework was fully penetrated by the physical network formed by complexation of chitosan (CS) and Fe^{3+}. Compared to other divalent and trivalent cations, Fe^{3+} was chosen to promote the metal-ligand bond's strength of PAA-Fe^{3+}-CS GPE, becaused of its larger coordination number and more stable metal-ligand bond ($(COO)_3Fe$)). Zhang et al. adopted a strategy of in-situ grown zeolitic imidazolate frameworks (ZIF-67) on cellulose nanofiber (ZIF-67@CF) by coordination with Co^{2+} ion into PEO to form the composite SPE (ZIF-67@CF/-PEO), synergistically enhancing the physical and electrochemical properties of SPE (Fig. 3e and f) [55]. The ZIF-67@CF/PEO SPEs exhibit a high ionic conductivity of 1.17 × 10^{-4} S cm^{-1} (30 °C), broadened electrochemical window (5.0 V), and enhanced breaking strength of 18.7 MPa.

Alaniz et al. synthesized a crosslinked SPE by using covalently bonded imidazole-containing ligands and polyvalent metal salts nickel (II) bis-(trifluoromethane sulfonimide) ($Ni(TFSI)_2$) [57]. Stronger binding strength of the metal-ligand complex formed a mechanically robust network with excellent self-healing properties. Sun et al. reported a self-healing and recyclable PU with outstanding mechanical strength, coordination crosslinking Zn^{2+} ions with poly(dimethylsiloxane) (PDMS)/polycaprolactone (PCL) [58]. The polymer exhibit a high breaking strength (~52.4 MPa) and toughness (~363.8 MJ m^{-3}). These ion coordination crosslinking strategies are expected to be widely used in the field of polymer electrolyte.

3.3. *Mechanically interlocked crosslinking*

Mechanically interlocked polymers (MIPs) work by interlacing two or more molecular structures into the entire polymer network to form a mesh structure. Such structures are not only physically highly stable, but also their shape and properties can be controlled by external stimuli such as stretching/compression. This strategy is often used to improve the mechanical properties and structural stability of electrolyte materials

[59–61].

Polyrotaxanes are representative structure of MIPs which are frequently reported due to their stable ring-shaped molecule structure, such as: (a) Cyclodextrin-based polyrotaxanes; (b) Crown ether-based polyrotaxanes; (c) Cyclophane cyclobis(paraquat-p-phenylene) tetrachloride (CBPQT(4+)-based polyrotaxanes [62,63]. The threaded host molecules shuttlecock in the ring structure. In addition, when movable host molecules are partially crosslinked, the networked MIP structure can exhibit excellent toughness and flexible properties due to the movable interpenetrating network. Kim et al. reported a mechanically tough SPE with superior ionic conductivity based on partially crosslinked polyrotaxane molecules with diisocyanate (Fig. 4a) [64]. The outstanding Li^+ conductivity ($\sigma = 5.93 \times 10^{-3}$ S cm^{-1} at 25 °C) and Li^+ transference number ($t_{Li}^{+} = 0.71$) are obtained. When coupling SPEs with $LiFePO_4$ (LFP) or $LiNi_{0.8}Co_{0.1}Mn_{0.1}O_2$ (NCM811) cells, an excellent fast charging capability (4C) can be achieved using the "built-in molecular shuttle" strategy (Fig. 4b).

During repeated insertion and extraction of Li^+, silicon suffers the huge volume changes and stress strain. This limit cycling life is caused by particle pulverization and unstable electrode-electrolyte interface. Polymer electrolytes and binders in silicon anode systems have similar characteristic requirements [65]. Choi et al. showed that the incorporation of 5 wt% polyrotaxane (PR) to conventional polyacrylic acid (PAA) binder imparts extraordinary elasticity and flexibility due to the mechanical interlocked crosslinking (Fig. 4c) [66]. This polymer binder keeps Si particles coalesced together, delivering a stable cycling life at a high areal capacities. The PR-PAA-Si preserved 2.43 mAh cm^{-2} after 150 cycles at 0.2 C with 91 % capacity retention.

To surmount the inherent trade-off between mechanical strength and stretchability of elastomers, Qu et al. proposed a supramolecular strategy of introducing a zipper-like sliding-ring mechanism in a H-bonds crosslinked PU network (Fig. 4d) [67]. A very small amount (0.5 mol%) The addition of 0.5 mol% of an external additive (pseudo [2]-rotaxane crosslinker) into PU can dramatically increase the maximum mechanical strength up to 45.06 MPa and maximum elongation up to 1890 %. This enhancement is attributable to that the unique molecular-level zipper--like ring-sliding motion efficiently dissipates mechanical. The molecular structure design ideas of many reported artificial SEI are also derived from SPEs. Liang et al. introduced a mechanically interlocked polymer chain network (^{DC}MIN) into the artificial solid electrolyte interphase (ASEI) to stabilize the Li metal/ASEI interface (Fig. 4e) [68]. The ^{DC}MIN crosslinked via efficient click reaction between the thiol unit of polydimethylsiloxane (PDMS) and the olefin of the hermaphroditic monomer exhibits flexibility and excellent mechanical properties (Fig. 4f). The crown ether in ^{DC}MIN not only interact with the dialkylammonium of a flexible chain, forming the energy dissipation behavior, but also coordinate with Li^+ to support the fast Li^+ transport in ^{DC}MIN. Therefore, a long-term 2800 h Li||Li symmetrical cycling (1 mA cm^{-2}) and an outstanding 5 C-rate of $LiFePO_4$ cells were achieved by ^{DC}MIN ASEI. The molecular design of mechanical interlocking materials provides broad

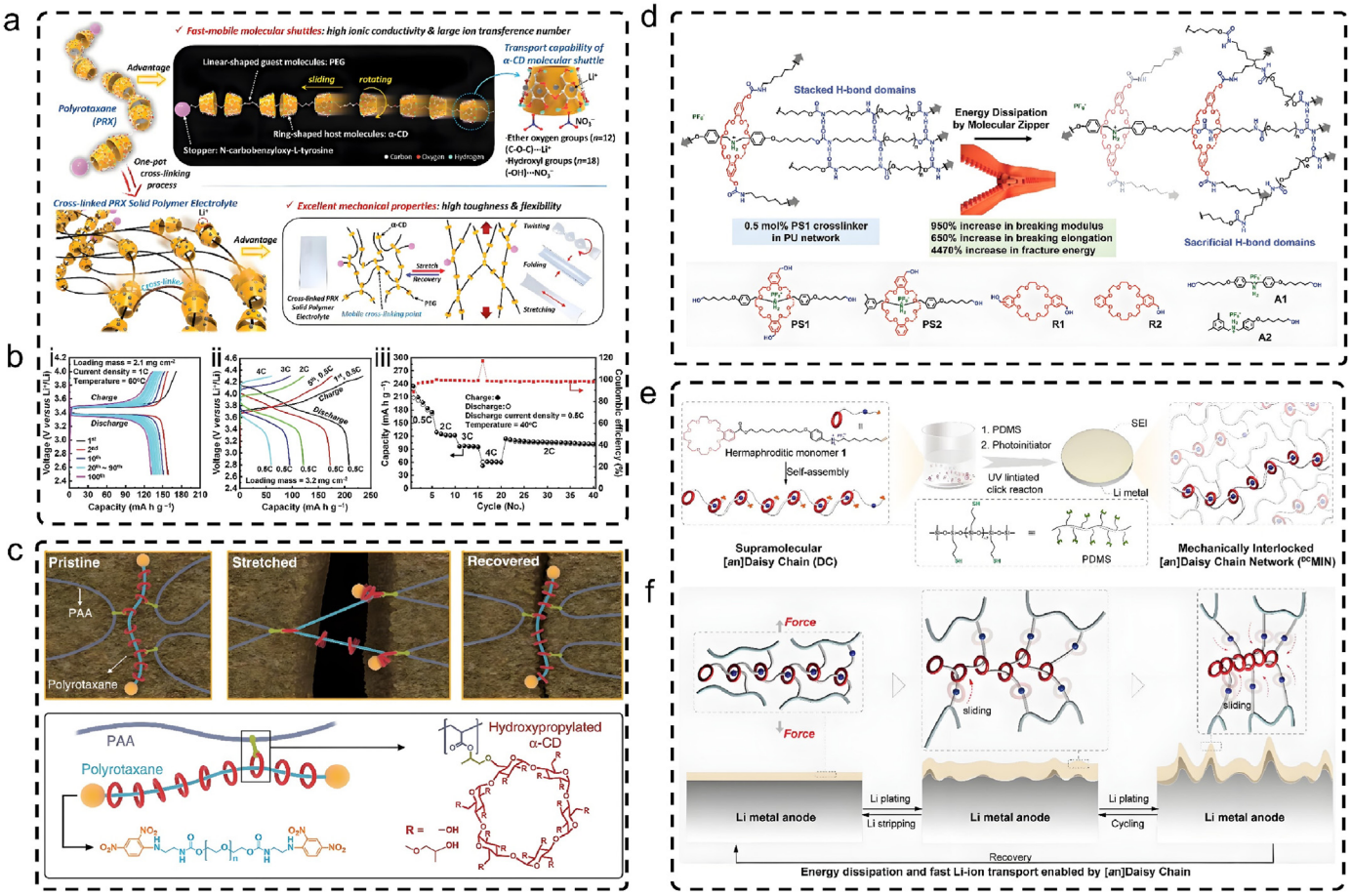

Fig. 4. Polymer electrolytes crosslinked by mechanically interlocking. a) Schematic of the built-in molecular shuttle design of crosslinked polymer. **b)** Charge-discharge profiles of LFP/PRX-SPE/Li cell **(i)**, charge-discharge profiles **(ii)** and rate performance **(iii)** of NCM811/PRX-SPE/Li cell [64]. Copyright 2021, Wiley-VCH. **c)** Interlocked Polyacrylic acid (PAA) with hydroxypropylated α-cyclodextrin to form a "molecular pulley structure" polymer [66]. Copyright 2017, American Association for the Advancement of Science. **d)** Zipper-like sliding-ring mechanism in a H-bonds crosslinked PU [67]. Copyright 2020, Wiley-VCH. **e)** Cartoon representation of the formation of [an]daisy chain (DC) and mechanically interlocked [an]daisy chain network. **f)** Mechanism of lithium metal anode protected by mechanical interlocking polymer [68]. Copyright 2024, Wiley-VCH.

application prospects in the field of ASEI and solid polymer electrolytes. To address the application problems of PEO electrolyte which were restricted by unsatisfactory Li $^{+}$ conductivity and a narrow electrochemical stability window. Yu et al. designed a self-assembled ether--based polyrotaxane based SPE by using different functional units and prepared by threading cyclic 18-crown ether-6 (18C6) to linear poly(-ethylene glycol) (PEG) via intermolecular H-bond and terminating with HDI [69]. The designed SPE has delivered an observably enhanced Li^{+} conductivity of ~3.5 × 10^{-4} S cm^{-1}, contributing to prolong the cycling life of SSLMBs when coupling with $LiFePO_4$ or $LiNi_{0.8}Co_{0.15}Al_{0.05}O_2$.

4. Chemical crosslinking

Chemical crosslinking refers to the process in which two or more molecular chains are connected by chemical bonds under the action of light, heat, high-energy radiation, mechanical force, catalyst and crosslinking agents to form a network structure polymer. The linear or mildly branched-chain macromolecules are transformed into a three-dimensional network structure to improve strength, heat resistance, chemical/electrochemical stability, anti-swelling and other properties. Chemical crosslinking strategy is one of the most popular strategies in the molecular structure design of polymer electrolytes, separator and binders in batteries. Due to the rich chemical reaction types and crosslinking reagents, this is very beneficial to the molecular structure design and regulation of crosslinked polymer electrolytes. According to the different commonly used crosslinking agents, it can be roughly divided into the following categories: small molecule crosslinker, inorganic particle crosslinker, organic/inorganic hybrid crosslinker, macromolecular crosslinker and biomass crosslinker.

4.1. Small molecule crosslinking

The small molecule crosslinking agent contains multiple functional groups, such as: (i) Vinyl monomers (Fig. 5a–e), (ii) Aldehyde monomer (Fig. 5f), (iii) Polyol monomer (Fig. 5g), (iv) Sulfhydryl monomers (Fig. 5h), (v) Glycidyl ethers (Fig. 5i–l) [70–77]. Because common one-dimensional linear polymer materials usually deliver unsatisfactory mechanical strength or without elasticity, the role of crosslinking agents is to generate chemical bonds between linear polymer chains to form a network structure, thereby improving the strength and elasticity of the polymer materials. This strategy has been frequently applied to the molecular structure design of SPEs in recent years.

Considering that the typical SPEs with easily oxidized oxygen-based groups exhibit unsatisfactory electrochemical stability window when matching with high voltage cathodes. Lee et al. reported an in-situ-formed elastomer SPEs (poly(ethylene glycol) diacrylate (PEGDA) and butyl acrylate (BA)) with a 3D crosslinked phase of ion-conductive plastic crystals (Fig. 6a) [78]. The authors developed a co-continuous structures of plastic-crystal-embedded elastomer SPE, which exhibited low activation energy (E_a = 0.13 eV), high Li^{+} conductivity (1.1 mS cm^{-1}) and Li^{+} transference number of 0.75. In addition, its mechanical strength effectively accommodated the stress-strain of Li anode during cycling. Chen et al. applied a polyfluorinated crosslinker to enhance resistance to electrochemical oxidation of SPEs due to introducing electron-withdrawing functional group (Fig. 6b) [79]. The SPE was crosslinked by three monomers of polyfluorinated crosslinker 2,2,3,3,4,4,5,5-octafluoro-1,6-hexanediol diacrylate (OFHDODA), 1-allyl-1-methyl-pyrrolidinium bis(trifluoromethanesulfonyl) imide ionic liquid (IL), and vinyl ethylene carbonate (VEC) by UV light polymerization. Young's modulus of the crosslinked P(IL-OFHDODA-VEC) was ~142 MPa, higher than that of the linear P(IL-VEC) (~27 MPa). With an excellent conductivity of 1.37 mS cm^{-1}, the Li|SPE|$LiNi_{0.5}Co_{0.2}Mn_{0.3}O_2$ cell (charging voltage 4.5 V) delivered a high capacity of ~164 mAh g^{-1} at 0.5 C with capacity retention of ~90 %.

Epoxy ring-opening is a kind of very attractive polymerization reaction, which is widely used in the synthesis of epoxy resins and in-situ polymerization of SPEs [84,85]. Chen et al. fabricated a fluorinated and crosslinked polyether-based SPE (FGPE), which was through in-situ cationic ring-opening polymerization of fluorinated monomer (trifluoropropene oxide (TFPO)) and four-armed cross-linker

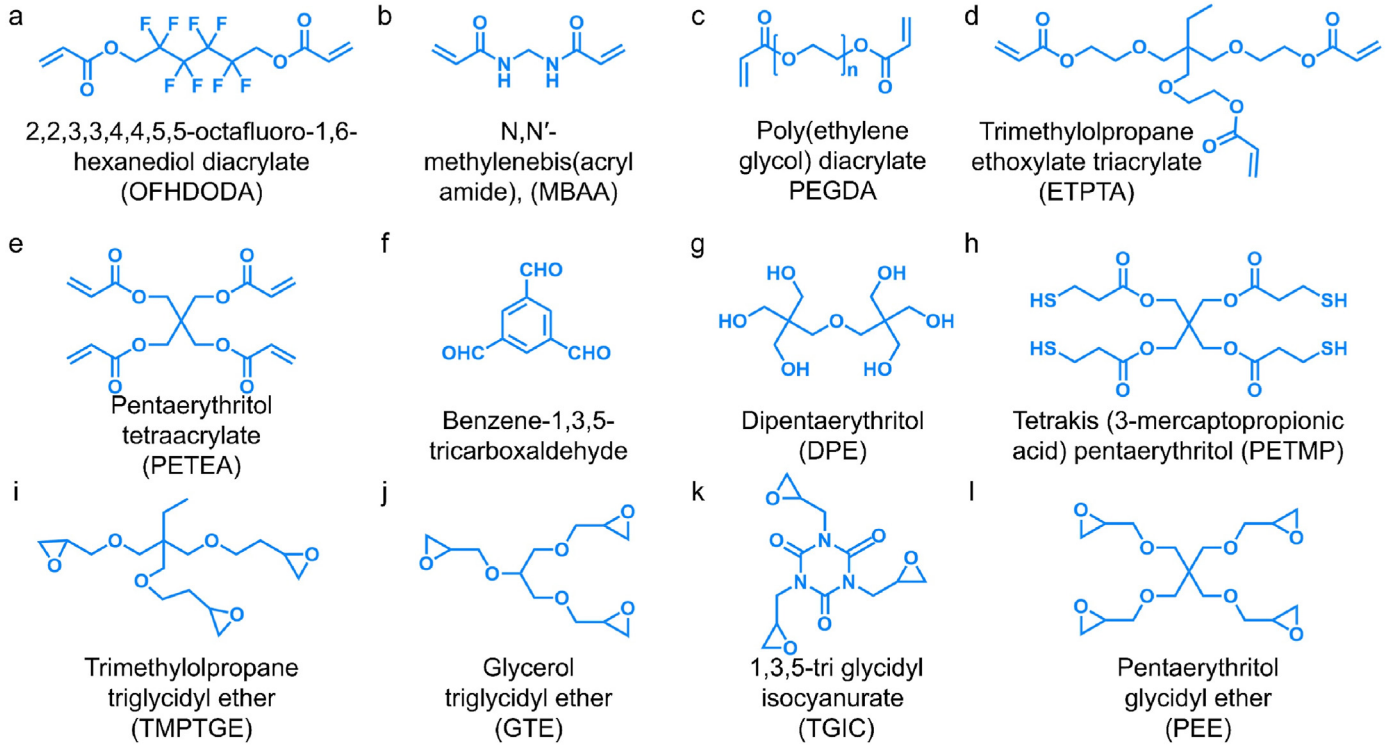

Fig. 5. Chemical structures of various common monomers. a-e) Vinyl monomers, **f)** Aldehyde monomer, **g)** Polyol monomer, **h)** Sulfhydryl monomers, **i-l)** Glycidyl ethers investigated in this study.

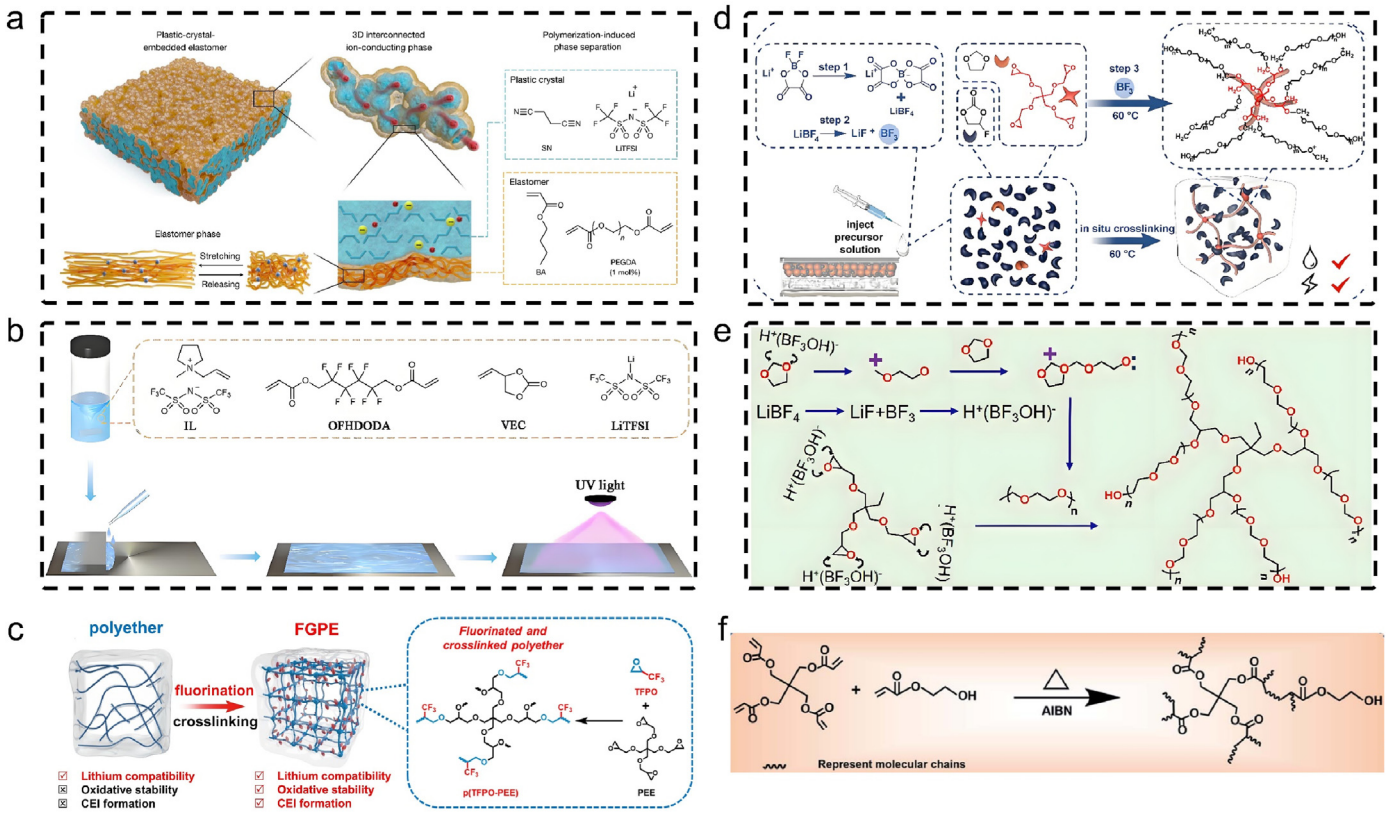

Fig. 6. Crosslinked polymer electrolyte constructed by monomer polymerization with multiple functional groups. a) Schematic illustration of the plastic-crystal-embedded elastomer electrolyte [78]. Copyright 2023, Nature Publish Group. **b)** Schematic illustration of the P(IL-OFHDODA-VEC) after UV light curing [79]. Copyright 2021, Nature Publish Group. **c)** The crosslinked polymer electrolyte was constructed by monomer polymerization with multiple functional groups [80]. Copyright 2024, Wiley-VCH. **d)** Schematic illustration of the crosslinking polymerization of PEE with DOL [81]. Copyright 2015, Elsevier. **e)** The crosslinked polymerization mechanism of DOL and TTE monomers initiated by $LiBF_4$ [82]. Copyright 2022, Elsevier. **f)** Synthesis of the PHGPE by reaction of PETEA with HEA [83]. Copyright 2022, The Royal Society of Chemistry.

(polyfunctional pentaerythritol glycidyl ether (PEE)) within the battery (Fig. 6c) [80]. This in-situ crosslinking method ensured interfacial contact of electrode/electrolyte and exhibited high voltage oxidation resistance (5.1 V), Consequently, due to the electron-withdrawing $-CF_3$ group and the LiF-rich SEI, the Li|FGPE|NCM622 SSLMBs demonstrated a long-cycling life of 1000 cycles with 78 % capacity retention, as well as the 18650-type cylindrical cells (1.3 Ah, 500 cycles) with high cathode loading (21 mg cm^{-2}). Chen et al. also constructed a 3D crosslinked SPE (PEE-DOL) based in-situ polymerization strategy. With the electrolyte solvent 1,3-dioxolane (DOL), the polyfunctional pentaerythritol glycidyl ether (PEE) with four epoxy groups was used as a cross-linker (Fig. 6d) [81]. A high Li^+ conductivity (~2.4 mS cm^{-1}) and oxidative stability (~4.5 V) are achieved. Moreover, due to the reduced desolvation energy of Li^+ and LiF-rich SEI, the Li||$LiFePO_4$ (LFP) and high-voltage Li||$LiNi_{0.6}Mn_{0.2}Co_{0.2}O_2$ (NMC622) achieved a long lifespan of 2000 and 300 cycles, respectively. Design of SPEs that combines ultra-thin thickness with high mechanical strength is essential to improve energy density and safety of SSLBs. Deng et al. reported an ultrathin (12 μm) crosslinked SPE for flexible SSLMBs by in-situ crosslinked polymerization of 1, 3-dioxolane (DOL), and trimethylolpropane triglycidyl ether (TTE) with $LiNO_3$ additive (Fig. 6e) [82]. The 3D crosslinked structure enabled the designed SPE with high Li^+ conductivity of 0.3 mS cm^{-1} and enhanced oxidation stability (4.9 V). The formative Li_3N/LiF-rich SEI promoted uniform Li deposition. The integrated $LiFePO_4$ pouch cell delivered high capacities retention (>90 %) and high operation safety during 2000 cycles of bending. Sun et al. synthesized a novel 3D crosslinked GPE by in-situ cross-linking reaction of pentaerythritol tetraacrylate (PETEA) and 2-hydroxyethyl acrylate (HEA) in commercial LE (Fig. 6f) [83]. The symmetric Li|GPE|Li cells delivered a long cycling life of 6000 h (1 mA cm^{-2}, 1 mAh cm^{-2}) and 7700 h (0.5 mA cm^{-2}, 2 mAh cm^{-2}). The wide electrochemical stability enabled the GPE with the ability to compatible with both NCM811 and sulfur cathodes.

4.2. *Inorganic particle crosslinking*

Organic/inorganic compound strategy by recombination inorganic fillers (e.g., Al_2O_3, ZrO_2 and SiO_2) or inorganic fast ionic conductor (e.g., $Li_{0.33}La_{0.557}TiO_3$, $Li_7La_{2.75}Ca_{0.25}Zr_{1.75}Nb_{0.25}O_{12}$ and $Li_{6.4}La_3Zr_2Al_{0.2}O_{12}$) with SPEs is widely applied to reduce crystallinity and increase Li^+ conductivity of SPEs [90–92]. Such overall improvements of electrochemical performances are generally attributed to the Lewis acid interactions between nanofiller and polymer/salt. Nanofillers involved in the polymer matrix are considered to introduce more nanofiller/polymer interfaces, reducing the crystalline of SPEs, promoting the dissociation of Li salts, and constructing high-throughput Li^+ transport pathway.

Therefore, polymers/nano-fillers interface, including the regulation of nanofiller size, concentration, and hybridization strategies, is key factor to fabrication of composite polymer electrolytes (CPEs). So far, various nanofillers of the CPEs have been investigated and reported. However, establishing a more powerful interaction relationship between the inorganic nanofillers and the polymer skeleton, rather than a single physical mixing with weaker interaction, is important to further promote the structural stability of the CPEs. Therefore, how to improve the dispersion of the nanofiller, prevent agglomeration or phase separation, increase the contact area of organic-inorganic interface, and increase the proportion of amorphous areas, is significantly conducive to the migration of Li^+. The chemical crosslinking between the polymer chains and inorganic nanofillers can significantly improve the mechanical strength

and electrochemical stability of the CPEs, thereby inhibiting the penetration of Li-dendrites, buffering the stress/strain caused by the volume expansion of cathode and anode materials, and ensuring the battery safety.

This strategy requires prior modification of specific functional groups on the surface of nanomaterials [93]. Archer et al. grafted oligomers with isocyanate group (−N=C=O) onto inorganic SiO_2 nanoparticles (Fig. 7a) [86]. The reaction between −N=C=O groups in poly(propylene oxide) (PPO) and hydroxyl (−OH) groups on the hairy silica (SiO_2−OH) nanoparticles form the crosslinked nanoparticle-polymer composite with urethane (−NH−COO−) groups. The obtained hairy nanoparticles are employed as crosslinkers, the homogeneous dispersion and arrangement

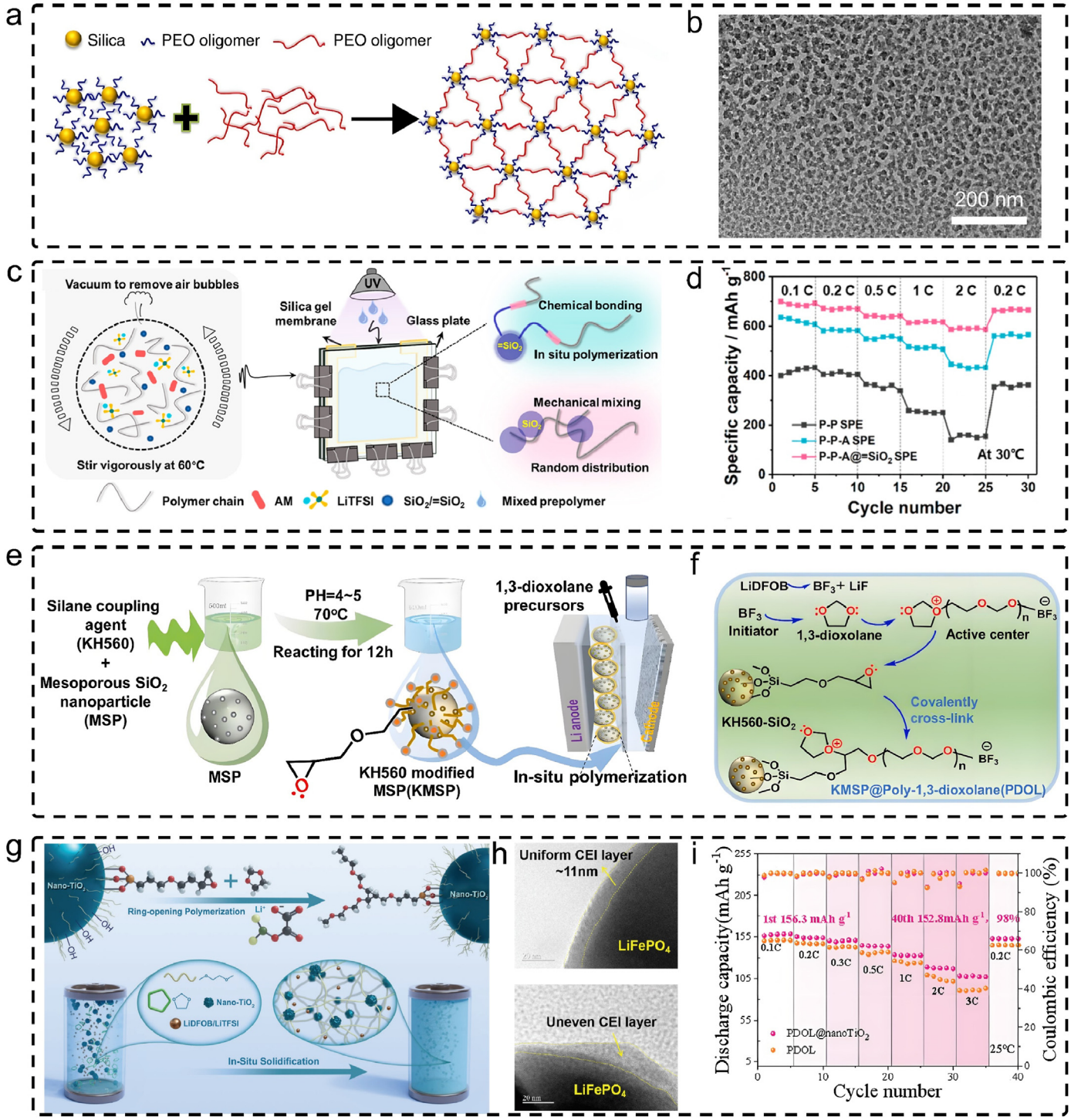

Fig. 7. Crosslinking polymerization of inorganic oxide nanomaterials with organic monomers. a) Scheme of synthesis process of the crosslinked nanoparticle-polymer composite. **b)** TEM image of the crosslinked SPE [86]. Copyright 2015, Nature Publish Group. **c)** Preparation route of P-P-A@SiO_2 SPE. **d)** Comparison of rate performance of solid-state battery at 30 °C [87]. Copyright 2021, American Chemical Society. **e, f)** Schematic illustration of composite electrolytes synthesized by crosslinking of end-epoxidized SiO_2 (KMSP) and 1,3-dioxolane (DOL) [88]. Copyright 2022, Elsevier. **g)** Schematic diagram of in-situ crosslinking of TiO_2 nanoparticle and DOL (PDOL@nanoTiO_2). **h, i)** Comparison of TEM images (h) and rate performance (i) of LFP|PDOL|Li and LFP|PDOL@nanoTiO_2|Li batteries [89]. Copyright 2022, Wiley-VCH.

of SiO_2 nanoparticles in the crosslinked polymer matrix was obtained from transmission electron microscopy (TEM) (Fig. 7b). The robust mechanical strength of CPE effectively inhibited Li-dendrite growth in SSLMBs. Wang et al. crosslinked modified silica and acrylamide (AM) with the poly(ethylene glycol) methyl ether methacrylate-poly(ethylene glycol) diacrylate (Fig. 7c) [87]. The multiple H-bonds of AM expand the single Li environment (Li···O−C) to three types (Li···O−C, Li···N−H, and Li···O=C), significantly improve the transfer efficiency of Li^+. The SiO_2 crosslinked CPE (P-P-A@SiO_2) assembled all-solid-state lithium-sulfur battery (S loading: 4.3 mg cm^{-2}) delivered the specific discharge capacity of 613 mAh g^{-1} even at 1 C at 30 °C (Fig. 7d). Cao et al. also prepared a novel crosslinked CPE based on poly(propylene oxide)-poly(ethylene oxide)-poly(propylene oxide) triblock polymer and modified nano-SiO_2 (Fig. 7e and f) [94]. The CPE exhibited high ionic conductivity of 1.32 mS cm^{-1} with an electrochemical stability window up to 6.5 V. The CPE delivered excellent mechanical stability (tensile elongation of 700 %). Li|CPE|$LiFePO_4$ delivered a high capacity of 160 mAh g^{-1} (0.2 C). Tian et al. proposed a highly stable CPEs (PDOL@nanoTiO_2) by crosslinking of nano-TiO_2 and DOL with a Li^+ conductivity of 1.74×10^{-3} S cm^{-1} and t_{Li}^+ of 0.725 (Fig. 7g) [89]. These properties enable the Li|PDOL@nano-TiO_2|Li symmetric battery keep stable cycling at 0.5 mA cm^{-2} for 1000 h. The $LiFePO_4$|PDOL@nanoTiO_2|Li cell exhibited a high capacity of ~143 mAh g^{-1} at 1 C, with an 90 % capacity retention (1000 cycles). The thinner (~11 nm) and uniform CEI after cycling formed by PDOL@nanoTiO_2 reduced the polarization of the battery, and inhibited the oxidative decomposition of the electrolyte (Fig. 7h).

4.3. Organic-inorganic hybrid crosslinking

Combining inorganic nano-fillers with SPEs is an effective approach to suppress the crystallization of polymers, promoting the ion transport capability of SPE. Unfortunately, these inorganic fillers with irregularly morphology and relatively weak polymer-fillers interaction result in aggregate and phase separation in the polymer matrix. Organic-inorganic hybrid nanomaterials, such as polyhedral oligomeric silsesquioxane (POSS) (Fig. 8a), ligands protected metal oxygen cluster (MOCs) (Fig. 8b and c), and metal-organic frameworks (MOFs), reveal more unique advantages. Benefited from their accurate structure parameter, adjustable surface functional groups and excellent dispersion, they are widely used in the field of crosslinked SPEs [95,96].

Hybrid polyhedral oligomeric silsesquioxane (POSS) is composed of Si-O interchangeably connected inorganic core skeleton, its shape is like a "cage", with a three-dimensional size of 1~3 nm. POSS/polymer hybrid material are recently developed as a kind of high-performance organic/inorganic hybrid materials with excellent thermal stability, mechanical properties and flame retardancy [102,103]. With multi-functional POSS

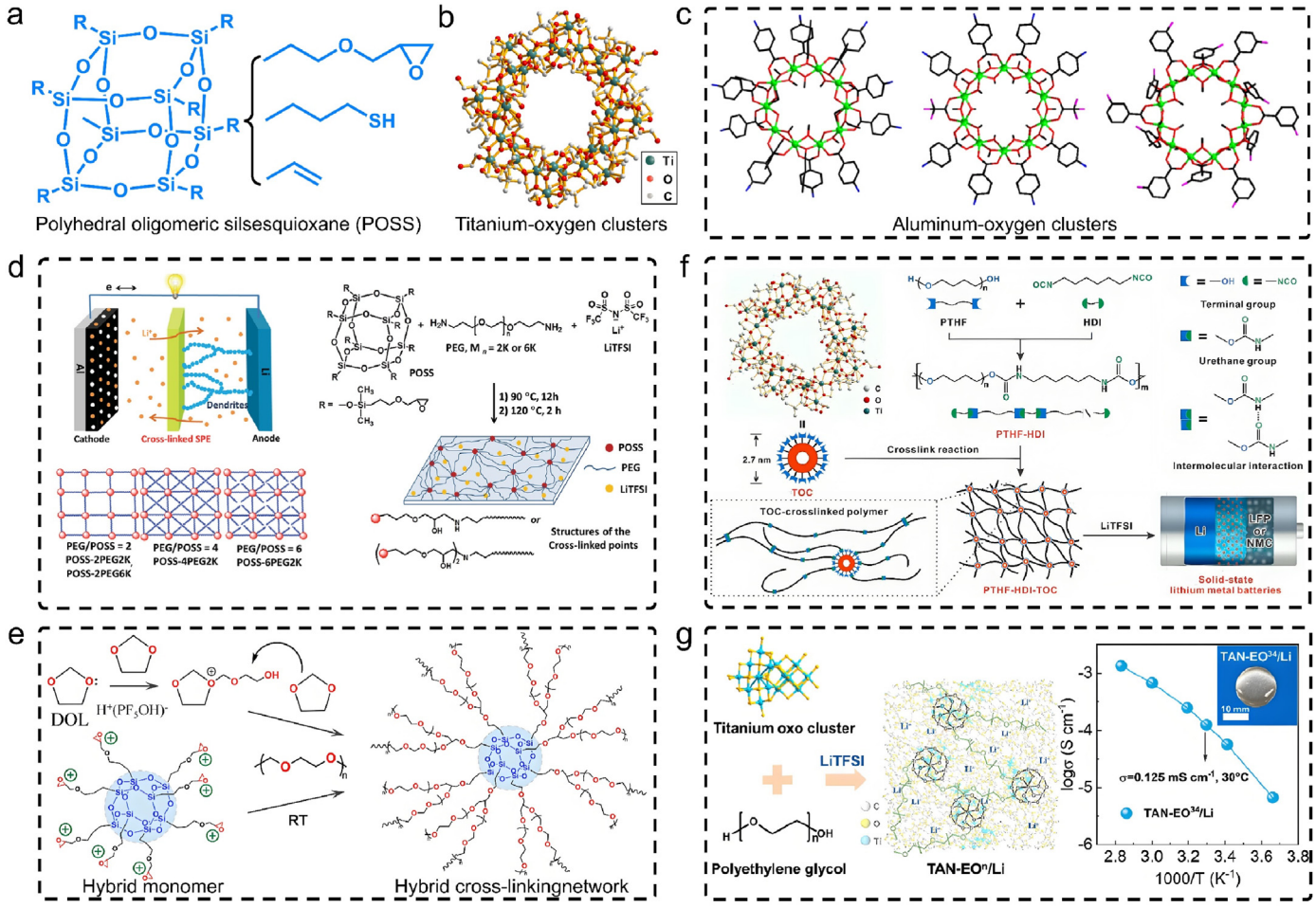

Fig. 8. Hybrid nanomaterials with multi-functional groups used as multi-site cross-linking reaction nodes. a) Molecular structure of polyhedral oligomeric silsesquioxane (POSS). **b)** Molecular structure of titanium-oxo clusters (TOC) [91]. Copyright 2021, The Royal Society of Chemistry. **c)** A summary molecular structure of 4-aminobenzoic molecular rings bridged with 4-aminobenzoic [97]. Copyright 2022, Wiley-VCH. **d)** Schematic illustration of SPE constructed by cross-linking POSS with amino modified PEG [98]. Copyright 2015, Wiley-VCH. **e)** Schematic illustration of the hybrid crosslinked SPE (POSS and DOL) by in-situ polymerization [99]. Copyright 2023, Wiley-VCH. **f)** Schematic illustration of the titanium-oxo clusters crosslinked SPE by cross-linking the −OH group functionalized Ti-oxo clusters with polyurethane [100]. Copyright 2023, Elsevier. **g)** Schematic of forming noncrystalline titanium alkoxide networks (TANs) with titanium-oxo clusters and PEG. **h)** Ionic conductivity of TAN/LiTFSI [101]. Copyright 2023, American Chemical Society.

inorganic component as the cross-linking agent, the inorganic phase and the organic phase are combined by strong chemical bonds, and it is easy to be synthesized with the polymer matrix by copolymerization, grafting and crosslinking. Li et al. reported a crosslinked SPE with organic/inorganic hybrid epoxy-modified POSS as crosslinker and amine-terminated poly(ethylene glycol) (PEG2000) as Li^+ conductor (Fig. 8d) [98]. POSS-PEG electrolyte with high ion conductivity (~0.1 mS cm^{-1} at room temperature) or (>1 mS cm^{-1} at 105 °C) and high breaking strength (33.6 MPa) was obtained. The Li|POSS-PEG|Li symmetric battery delivered the cycling stability of 2600 h (0.3 mA cm^{-2}). Zhu et al. proposed a strategy of organic/inorganic hybrid crosslinked polymer electrolyte (HCPE) via in-situ polymerization of DOL and glycidyl ether oxypropyl cage polyhedral silsesquioxane (POSS) as a crosslinking agent and hybrid center [99]. The non-flammable HCPE delivered superior ionic conductivity of 2.22 × 10^{-3} S cm^{-1}, ultrahigh Li^+ transference number of 0.88, and wide electrochemical stability window of 5.2 V (Fig. 8e). The assembled Li|HCPE|$LiFePO_4$ batteries delivered long-cycling life over 600 cycles at 2 C and high capacity retention of 92.1 %. Wei et al. developed a series of organic/inorganic hybrid star-shaped crosslinked SPEs by free radical polymerization using POSS with eight vinyl (−C=C) functional corner groups, while poly(ethylene glycol) methyl ether methacrylate (PEGMEM) was applied to dissolve lithium salt [104]. The SPEs exhibited a high Li^+ conductivity of ~1.1 × 10^{-4} S cm^{-1} (25 °C) and t_{Li}^+ of 0.35.

Compared with the conventional inorganic fillers (e.g., TiO_2, Al_2O_3 and SiO_2) with non-uniform sizes and high aggregation tendency, metal-oxo clusters (e.g., Ti-oxo, Al-oxo, Zr-oxo and lanthanide-oxo clusters), as an important class of organic-inorganic hybrid crystalline nanomaterials with uniform structural parameters, act as a bridge connecting organic molecule and inorganic nanoparticle/bulk material. From the perspective of structural characteristics, metal-oxo cluster with regulable functional groups of surface ligands (e.g., $-NH_2$, −OH and −COOH) can be regarded as the multi-site crosslinked reaction sites, exhibiting the significant advantages to rationally design the molecular structure of crosslinked polymers at the atomic level (Fig. 8b and c) [97,105,106]. For example, Zheng et al. reported a kind of titanium-oxo clusters (TOC) which possessed controllable surface ligand with functional groups (e.g., ethanol, glycerol, and polyethylene glycol), so they can act as crosslinked reaction node to fabricate the nanofiller-crosslinked hybrid SPEs [91,105]. Therefore, Fang et al. designed the −OH functionalized Ti-oxo clusters (TOC) crosslinked polyurethane based SPEs (PTHF-HDI-TOC/LiTFSI) to construct robust SSLMBs (Fig. 8f) [100]. A wheel-like TOC was synthesized with a formula of $Ti_{32}O_{16}(OCH_2CH2O)_{32}(R\text{-}COO)_{16}(OCH_2CH_2OH)_{16}$ (R = t-butyl). The crosslinked PTHF-HDI-TOC/LiTFSI showed the enhaned room-temperature ionic conductivity (1.34 × 10^{-4} S cm^{-1}), mechanical strength (10.63 MPa) and

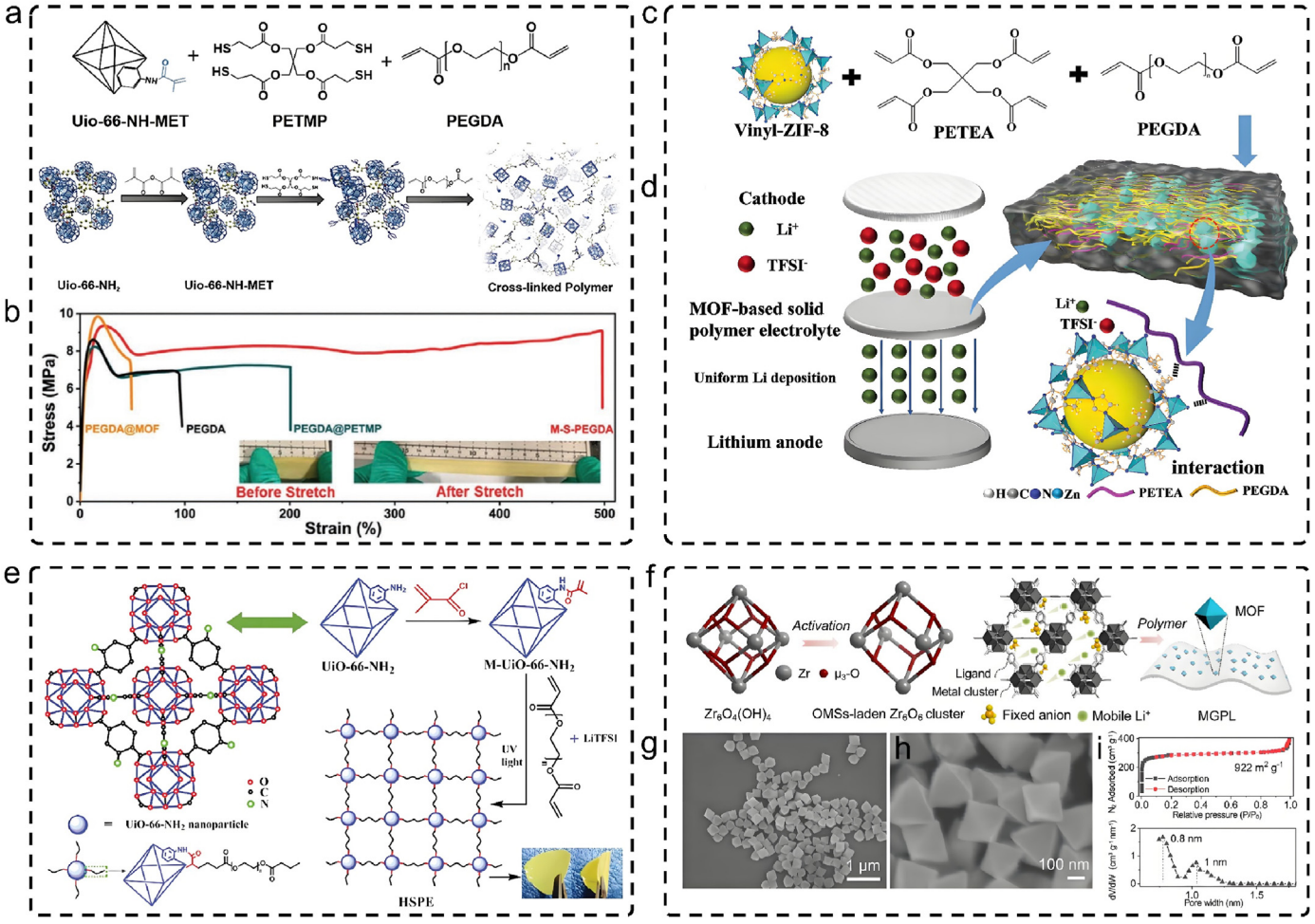

Fig. 9. MOF materials with multi-functional groups used as multi-site cross-linking reaction nodes. a) Chemical precursors and synthesis scheme for the crosslinked polymer electrolyte by UIO-66-NH_2. **b)** Stress-strain comparison curves of various polymers [108]. Copyright 2020, Wiley-VCH. **c)** Main chemicals for the synthesis of crosslinked polymers (P-PETEA-MOF). **d)** Structure illustration of Li^+ conduction in P-PETEA-MOF [109]. Copyright 2023, Wiley-VCH. **e)** Synthesis of the cross-linked MOFPEGDA-based SPE [110]. Copyright 2018, The Royal Society of Chemistry. **f)** Illustrative drawings of Zr-based MOF (UiO-66) facilitating Li^+-ion conduction in gel SPE. **g, h)** SEM images of UiO-66. **i)** N_2 isotherms (top) and corresponding pore size distribution (bottom) of activated UiO-66 [111]. Copyright 2020, American Chemical Society.

t_{Li}^{+} (0.6). The SSLMBs assembled with $LiFePO_4$ or $LiNi_{0.8}Mn_{0.1}Co_{0.1}O_2$ cathodes exhibited enhanced capacities and cycling life. Xie et al. proposed a novel crosslinked metal-alkoxy-terminated SPE by precisely controlling the content of H_2O as an initiator (Fig. 8g) [107]. nano-Al-O nanoclusters can serve as crosslink nodes to enhance PEO chains to 8×10^6 g mol^{-1}. The crosslinked polymer network incorporated a high concentration of plasticizers over 75 wt%, still maintained excellent elasticity and breaking strength. The SPE delivered high Li^+ conductivity (1.41 mS cm^{-1} at 30 °C) and a stable electrochemical window (>4.8 V). Besides, the Li||$LiFePO_4$ delivered a long cycling life over 1000 cycles at 1 C.

Metal-organic frameworks (MOFs) materials have attracted much attention as functional nanofillers due to their precise crystal structure and geometry [112,113]. Specially, zirconium-based MOFs are one of the most robust materials due to their strong coordination bonds, which have been widely used in the field of SPEs. Sun et al. designed a new SPE which was enabled by chemically crosslinked MOFs (UIO-66), tetrakis(3-mercaptopropionic acid) pentaerythritol (PETMP), and poly(-ethylene glycol) diacrylate (PEGDA) (Fig. 9a) [108]. The MOFs were connected with PEGDA through PETMP, leading to a high ionic conductivity of ~0.23 mS cm^{-1}. The −C−S−C− covalent bonds showed an enhanced breaking strength (9.4 MPa) and toughness (~500 %), balancing the trade-off between electrochemical and mechanical performance of SPEs (Fig. 9b).

Fu et al. designed a novel hybrid SPE by the crosslinked of vinyl-MOFs (Vinyl-ZIF-8), pentaerythritol tetraacrylate (PETEA), and polyethylene glycol (ethylene glycol) diacrylate (PEGDA) (Fig. 9c and d) [109]. The ionic conductivity was as high as ~0.65 mS cm^{-1}. The formation of crosslinked fameworks enhanced the mechanical strength of SPEs (tensile strength of 1.85 MPa and elongation of 45.4 %). Zhang et al. designed a free-standing, flexible and homogenous hybrid SPE membrane by chemically linked with the double bonds decorated MOF (UiO-66-NH_2) as crosslinking center (Fig. 9e) [110]. The forming space grid structure provid additional transport channels for Li^+. PEGDA not only can conduct Li^+ but also constructing a crosslinked structure.

Lu et al. employed a Zr-based MOF possessing open-metal sites (OMSs) as the crosslinker for GPE (Fig. 9f) [111]. their selected MOF provided Lewis acidity that can readily immobilize anions and facilitate Li^+ conduction, affording high Li^+ conductivity (1 mS cm^{-1}), high t_{Li}^{+} (0.66), and low activation energy (<0.1 eV). The UiO-66 (Fig. 9g and h) exhibited an uniform morphology in scanning electron microscopy (SEM) image. The UiO-66 showed a huge surface area of 922 m^2 g^{-1} (Fig. 9i). Huang et al. proposed a novel strategy to fabricate crosslinked MOFs chains to build a continuous Li^+ transport path [114]. $-SO_3H$ groups modified MOF (Zr-BPDC-2SO_3H) can facilitate the ion transport along the pore channels. The crosslinked SPE exhibited a high Li^+ conductivity of 0.79 mS cm^{-1} and wide electrochemical stable window (5.10 V).

4.4. Macromolecular crosslinking

So far, numerous semicrystalline/amorphous, inexpensive and convenient polymers with typical straight-chain macromolecules have been studied as the base materials of SPEs, including polyethylene oxide (PEO), poly (methylmethacrylate) (PMMA), poly(acrylonitrile) (PAN), poly(vinyl chloride) (PVC), polyvinyl alcohol (PVA), poly(acrylic acid) (PAA), poly(vinylidene fluoride) (PVDF), poly(vinylidene fluoride-hexafluoropropylene) (PVDF-HFP) [115–118]. In general, lithium salts are dissolved in these polymers with polar group (e.g., −O−, =O, −S−, −N−, −P−, −C=O, and −C ≡ N) to improve the Li^+ conductivities of SPEs. Nevertheless, these conventional polymers are still suffered from the lower Li^+ transference number and conductivity at room temperature due to the high crystallinity. Besides, their one-dimensional linear structure results in limited mechanical strength.

By introducing crosslinking agents, the single straight chain is transformed into a three-dimensional crosslinked network, which is a very effective strategy to solve the above problems in the field of SPEs. Wang et al. prepared a crosslinked polyurethane electrolyte (HPU) by the reaction of hyperbranched polyethylene glycol (HPEG) with isophorone diisocyanate (IPDI) in the presence of LiTFSI and PryTFSI (Fig. 10a) [119]. The obtained HPU electrolyte showed obvious low crystallization due to the hyperbranched polyurethane and ionic liquid, delivering a high Li^+ conductivity of 4.0×10^{-4} S cm^{-1} with a electrochemical stable window of 4.95 V so HPU can couple with various electrodes including $LiFePO_4$ (LFP), $Li_4Ti_5O_{12}$ (LTO) and $LiNi_{0.8}Co_{0.1}Mn_{0.1}O_2$ (NCM811). The high-voltage NCM811 and LTO-based cells exhibited 440 cycles at 0.2 C. Zhou et al. proposed a poly(ethylene oxide)-polyacrylonitrile (PEO-PAN) crosslinked SPEs, PAN nano-fibers act as crosslinker (Fig. 10b) [120]. This structure provided enhanced Li^+ conductivity, excellent mechanical properties, and inhibition of lithium dendrite growth, it also delivered the ability to inhibit polysulfide shuttling due to the strong polysulfide adsorption of C=N−O functional groups, improving the cycling stability and rate performance of Li-S batteries [124–126]. Zhu et al. reported a crosslinked SPE (SCOF-PEP-PEA) by using covalent organic framework (COF) containing abundant allyl groups (SCOF) [118]. Benefitting from the 3D crosslinked structure and abundant lithiophilic groups, the obtained SPE exhibited high mechanical strength (AFM Young's modulus: 453 MPa), Li^+ conductivity (4.0 mS cm^{-1}) and t_{Li}^{+} (0.82). As a result, the Li|SPE|$LiFePO_4$ full cell shows excellent rate capacity of 141 mAh g^{-1} (1 C).

Yan et al. synthesized a new type of polyurethane binder (PEI-HDI) by the polymerization of HDI with polyethylenimine (PEI) used for sulfur cathode binder (Fig. 10c) [121]. When compared to the traditional PVDF binder, the PEI-HDI with $-NH_2$ groups and crosslinked structures, provided the strong ability anchoring polysulfide, remarkably prolonged the cycling life of Li-S batteries (capacity retention of 91.3 % for 600 cycles). Wang et al. developed crosslinked polyethylene glycol-based resin (cPEGR) by ring-opening reaction of PEGDE with epoxy groups and PEA with $-NH_2$ (Fig. 10d) [122]. The GPE with LE (1 M $LiPF_6$ in DMC: FEC) achieved an ionic conductivity (7.0×10^{-4} mS cm^{-1}). LCO||Li cells with the GPE exhibited long cycling performances with a cut off voltage up to 4.35 V. Silicon is a promising anode material for Li-ion batteries. However, its large volume changes during cycling pose a great challenge for fabricating stable electrodes. Wang et al. designed polymer binder crosslinked by poly(acrylic acid)-poly(2-hydroxyethyl acrylate-co-dopamine methacrylate) (Fig. 10e) [123]. Its crosslinked famework with hard-soft chains and self-healing ability not only provided enough mechanical strength but also buffered the volume change of Si anode. Therefore, the molecular structure design of binders is very enlightening for solid electrolytes, especially when matching thick electrodes with high electrode loading [127].

4.5. Biomass crosslinking

Notably, a wide variety of biomass materials (e.g., starch, cellulose, lignin, chitin, proteins, and low-molecular-weight sugars) in nature provide an ideal source and templates for multifunctional materials. (Fig. 11a) [132–134]. Biomass is actually a class of biological macromolecules or carbohydrates with a variety of microstructure and rich functional groups, which provides more opportunities for its compatibility with SPEs. The biomass skeleton is thought to reduce polymer crystallinity, promote lithium salt dissociation, and construct new fast ion transport channels. And it can cope with the expansion of electrode volume during cycling. Most importantly, macromolecular biomass can directly replace industrial fossil-derived polymers, offering attractive prospects for the development of green high-performance SSLBs. Recently, more and more attention has been paid to the study of the biomass based SPEs.

As the most widely distributed and abundant biomass in nature, The raw materials of cellulose are mainly from wood, cotton, wheat grass, straw, reed and hemp. Despite its many attractive properties, cellulose still faces many inherent drawbacks, such as being insoluble in most

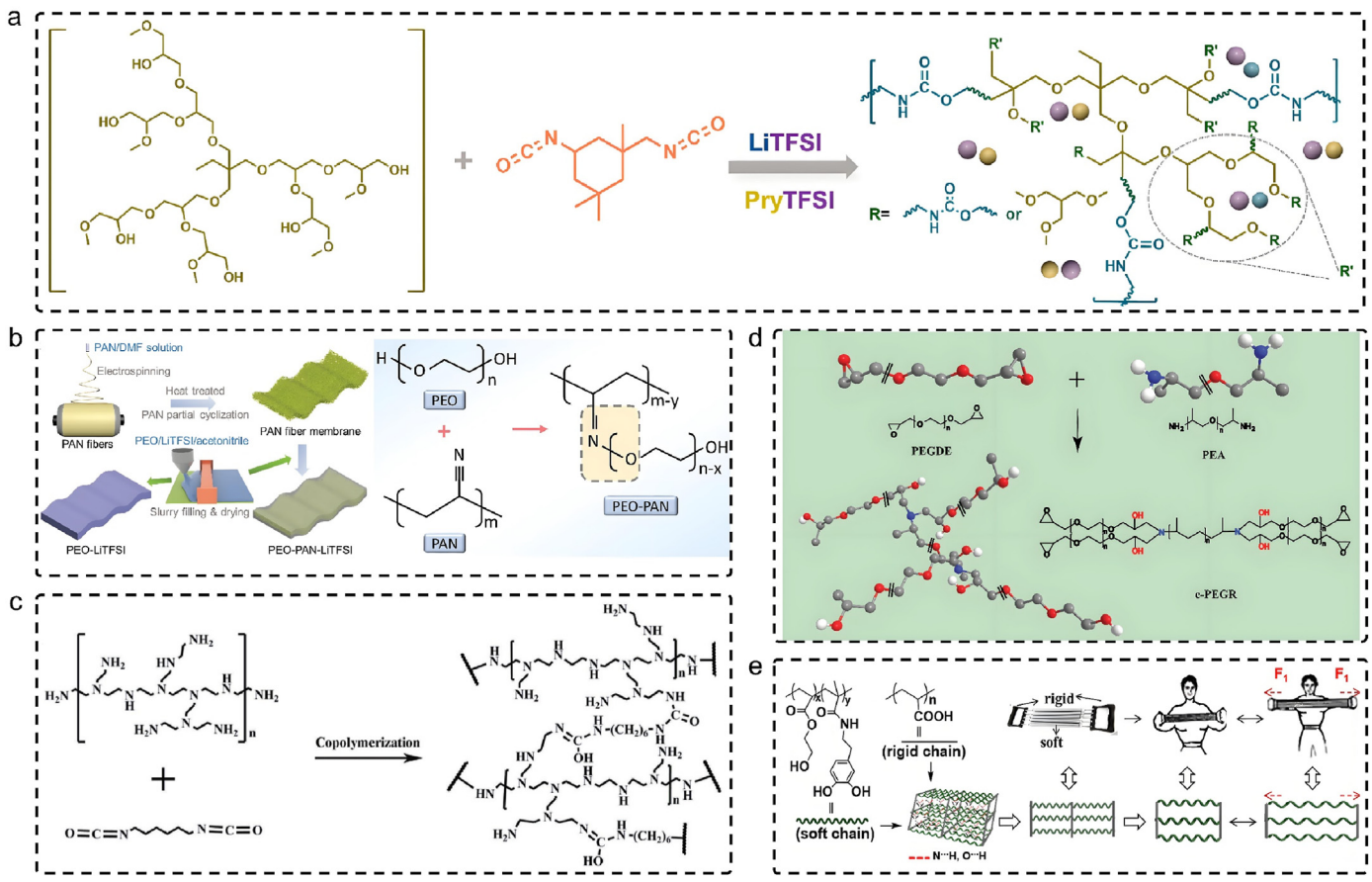

Fig. 10. Polymer electrolytes constructed by chemical crosslinking between macromolecules. a) The preparation of the hyperbranched cross-linking polyurethane electrolyte by the reaction of hyperbranched polyethylene glycol (HPEG) and IPDI [119]. Copyright 2024, Elsevier. **b)** Illustration of the preparation process and crosslinking mechanism of the PEO-PAN-LiTFSI electrolyte [120]. Copyright 2022, Wiley-VCH. **c)** Synthesis scheme of AFG binder by copolymerization of PEI with HDI [121]. Copyright 2017, Wiley-VCH. **d)** Crosslinked polyethylene glycol-based resin (cPEGR) was developed by ring-opening reaction [122]. Copyright 2017, Wiley-VCH. **e)** The spring expanders model of P(HEA-co-DMA) and PAA [123]. Copyright 2018, Elsevier.

solvents. Therefore, the cellulosic biomass need to be dissolved in solvents to obtain functionalized films and gels [135,136]. This benefits from the three active hydroxyl groups (−OH) on the glucose unit of cellulose can be modified by etherification, esterification and other methods, grafting or crosslinking of the polymer to increase their solubility. These modification strategies drastically improve the solubility of cellulose. Cellulose acetate (CA), cellulose acetate butyrate (CAB), methyl cellulose (MC), ethyl cellulose (EC) and hydroxy ethyl cellulose (HEC) are cellulose derivatives. Cyclodextrin (CD) is also a commonly used biomass material, which is mainly divided into α-cyclodextrin (α-CD), β-cyclodextrin (β-CD) and γ-cyclodextrin (γ-CD) (Fig. 11b) [128]. It is possible to chemically modify cyclodextrin molecules by grafting functional groups or cross-linking cyclodextrins to polymers.

In order to improve the functionality of natural cellulose and broaden its application range in the field of energy storage materials, modification of cellulose is a sensible and effective strategy. Chen et al. chemically modified the cellulose by allyl chloride in NaOH/urea solution (Fig. 11c) [129]. The allyl groups can crosslinked to enhance the mechanical properties and reduce the crystallinity of the SPE. Methyl cellulose (MC) was selected to react with acryloyl modified cellulose (AC) due to its excellent film forming ability and ability to absorb electrolyte due to the substitution of some hydroxyl groups by methoxy groups. Because cross-linking is an effective way to improve the mechanical and electrochemical properties of biomass-based SPEs. Considering the poor mechanical properties of starch, it is difficult to form a self-supporting film when used as a polymer substrate. Wang et al. prepared a novel biomass based SPE by react corn starch with g-(2,3-epoxy–propoxy) propyl trimethoxysilane and other coupling agents (Fig. 11d and e) [130]. The starch based SPE with 40 % LiTFSI content was used to construct high-energy density solid-state Li-S battery. The obtained SPE exhibits high ionic conductivity (0.34 mS cm^{-1} at 25 °C) and high t_{Li}^{+} (0.80). The Li-S battery delivered a high capacity of 864 mAh g^{-1} for 100 cycles. The rapid advances of cellulose-based SPEs has significantly reduced the cost of safe energy storage devices. Fang et al. reported a dynamic network of imidazolium bonds based on soy protein isolate (SPI) polymer electrolyte, which is recyclable and self-healing (Fig. 11f) [131]. This pliable covalently cross-linked network polymer can be reshaped and recovered at differenth temperatures (up to 100 °C), which helps achieve the recycling of energy materials. The addition of LiTFSI resulted in a conductivity of more than 0.33 mS cm^{-1} for the obtained SPE.

5. Summary and prospects

In summary, this review presents an overview of crosslinked SPEs by critically summary and analysisthestructure type of crosslinked polymer chain, and effective strategies to achieve the collaborative promotion of enhancing the ionic conductivity, ion transference number, mechanical properties, thermal stability, and interfacial electrochemical stability. The unique architectures of Physical crosslinking and chemical crosslinking strategies are classified in detail and discussed. In contrast to linear polymers, Spatial structure of 3D crosslinked polymer can effectively weaken T_g and crystallinity of polymer chains, endowing them with higher thermal motility and larger amorphous area. Nevertheless,

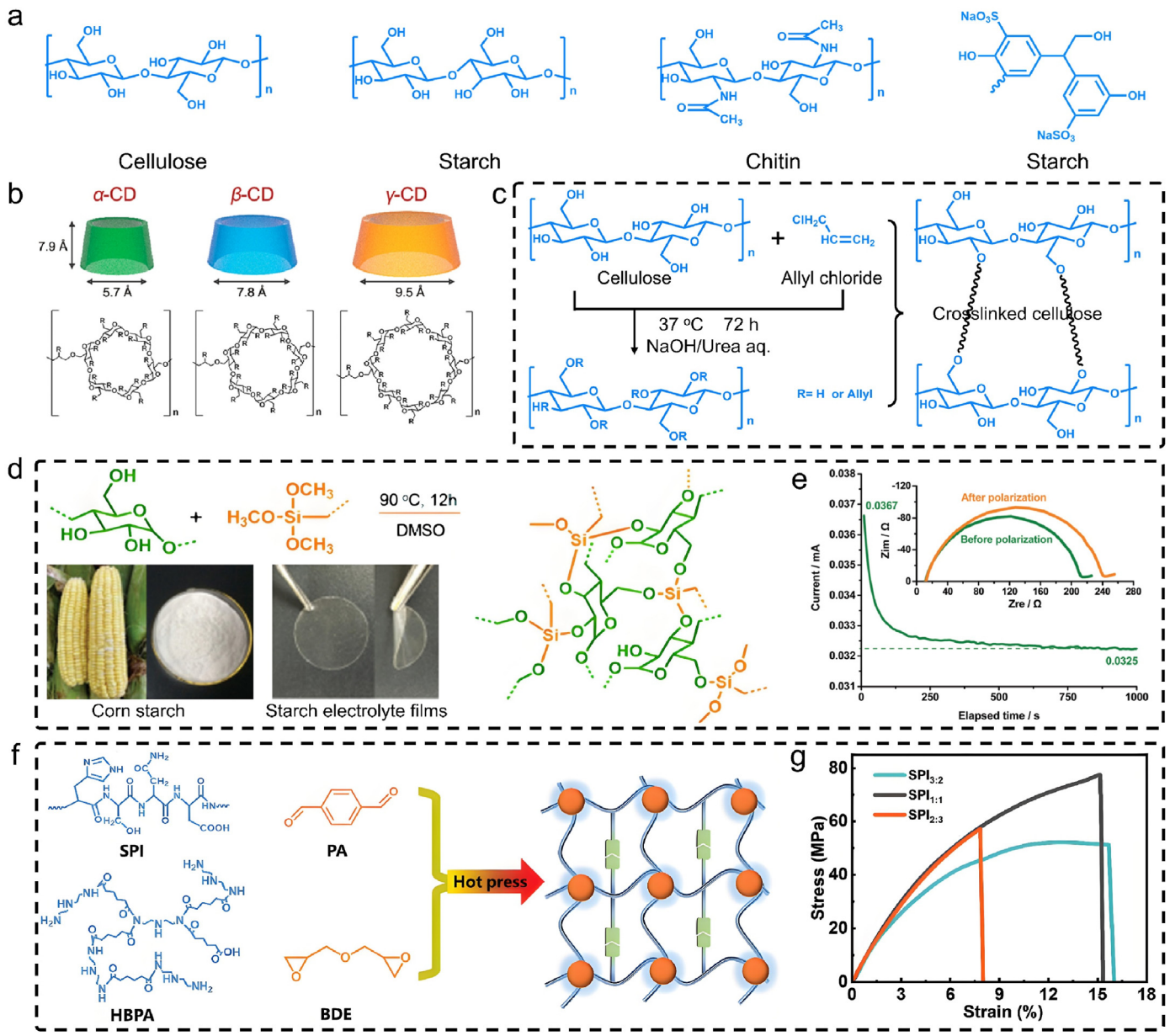

Fig. 11. Crosslinked polymer electrolytes constructed from biomass materials. a) The molecular structures of common biomass materials which are used to construct SPEs. **b)** Chemical structures of hyperbranched α-, β-, and γ-CD (cyclodextrin) [128]. Copyright 2015, American Chemical Society. **c)** Allylation of cellulose and crosslinking mechanism of allyl-modified cellulose [129]. Copyright 2020, Elsevier. **d)** Preparation of starch hosted electrolyte films. Inset: Images of the transparent and flexible electrolyte films with LiTFSI. **e)** Chronoamperometry of the Li|Starch + LiTFSI|Li cell. Inset: AC impedance spectra of the cell [130]. Copyright 2016, The Royal Society of Chemistry. **f)** The soy protein isolate (SPI) based matrix were crosslinked by PA and BDE. **g)** The stress-strain curve of SPI-based vitrimers [131]. Copyright 2022, Wiley-VCH.

there are still many potential problems to be solved and many exciting opportunities to be discovered in the commercialization of SPEs.

Therefore, in order to further improve the performance of crosslinked polymer electrolytes in high-safety solid-state batteries, we propose the following research directions.

5.1. Improving the high voltage electrochemical stability of the crosslinked SPEs

High-voltage solid-state lithium batteries are considered to be one of the most promising directions for research due to their high safety and energy density (Fig. 12a). Although significant research progress has been made in SPEs development, the oxidative decomposition/evolution (4.3–4.8 V) of the SPEs can directly affect the evolution of the internal interface of the battery and the cycle life, this challenge is further exacerbated by the high reactivity and structural instability between high-voltage cathode and electrolyte materials. Therefore, selecting monomers with high lithium salt solubility and high voltage tolerance will be the key research target in the future. Theoretical calculations can also play a more prominent role in this regard.

5.2. Developing more simple and controllable synthesis strategy for crosslinked polymer electrolytes

Tunable and controllable architecture offer crosslinked polymer a set of intriguing properties such as self-healing, shape memory and excellent stress-strain properties. Synthesizing crosslinked polymer electrolytes with highly tunable degree of polymerization, dielectric properties and

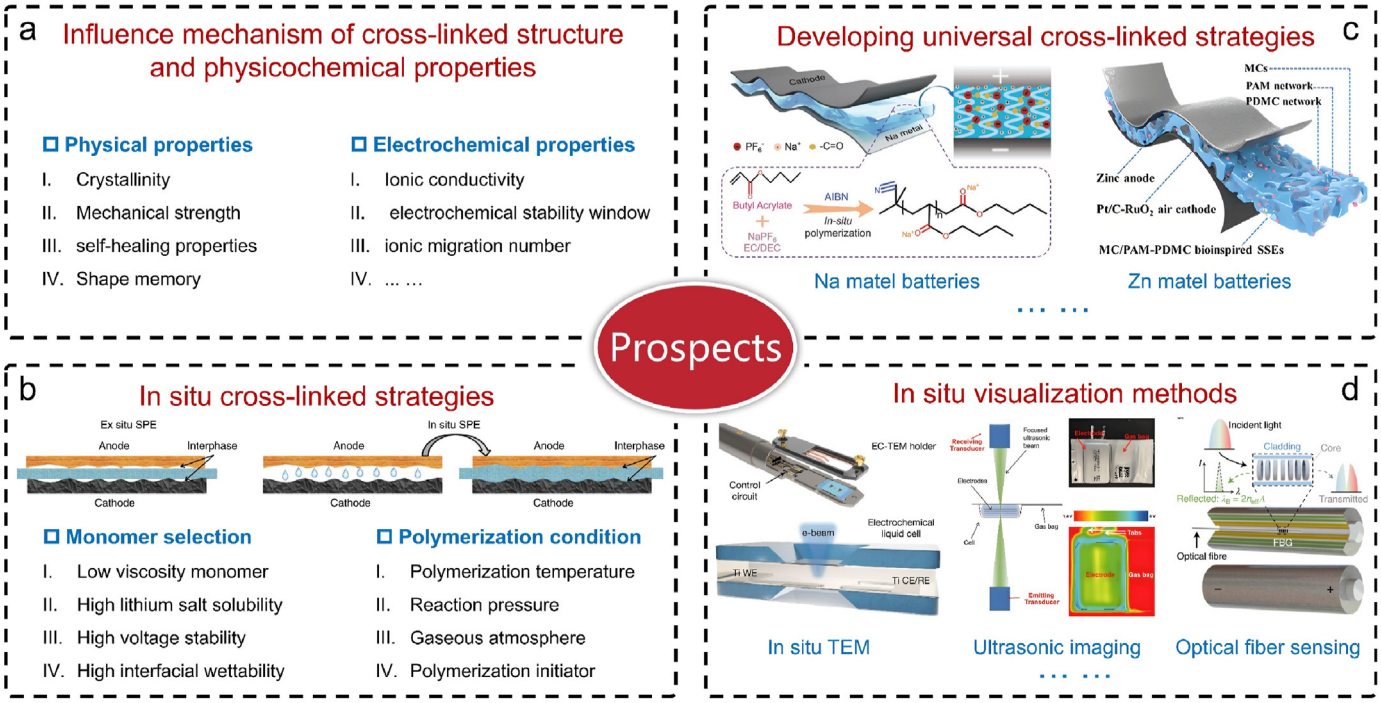

Fig. 12. The suggestion of the following research directions for further improving the performance of crosslinked SPEs in solid-state batteries. a) Influence mechanism between crosslinked structure and physicochemical properties. **b)** Developing in-situ crosslinked polymerization methods for future commercialized production [137]. Copyright 2019, Nature Publish Group. **c)** Developing universal cross-linking synthesis strategies adapted to multiple energy storage fields [138]. Copyright 2022, Nature Publish Group. **d)** Understanding the electrochemical properties of crosslinked SPEs by advanced in-situ characterization techniques [139–141]. Copyright 2021, Nature Publish Group. Copyright 2020, Elsevier.

crystallinity still faces difficulties to date. Moreover, crosslinkers with more functional characteristics need to be developed, the synthesis route should be enough environment-friendly low-cost precursors and mild reaction conditions are advisable for large-scale manufacturing of crosslinked SPEs. Unsatisfactory synthesis suggests that one fails to tailor SPEs with precise synthesis at the molecular level and to achieve physicochemical and electrochemical properties optimization. Thus, there is much room for performance improvement. Further studies are needed to design, controlled synthesis and characterization of crosslinked SPEs.

5.3. Developing in-situ crosslinked polymerization methods for future mass production

In-situ polymerization process for SSPLBs has been identified as one of the most promising strategies for solid-state polymer lithium batteries (SSPLBs) scale-up manufacturing, effectively solving the problems of interfacial contact and excessive thickness of SPEs. Besides, the in-situ polymerization economized the complex processes of polymer dissolution, film drying and laminated assembly process of the ex situ strategy, which effectively reduces the cost and is compatible with the existing battery production processes. However, most of the current studies on in situ polymerization have been based on coin cells at the laboratory level, while practical pouch cells have been much less studied. There is a huge difference between laboratory level coin SSLBs and practical pouch SSLBs. Moreover, in-situ polymerization process puts forward more requirements on the viscosity and solubility of monomers (Fig. 12b) [85, 142].

5.4. Developing universal cross-linking synthesis strategies adapted to other energy storage fields

Crosslinked polymer electrolytes have a wide range of applications, and the ion transport mechanisms in polymers have many similarities. Large-scale production of crosslinked polymer electrolytes indeed faces challenges (e.g., Large-scale synthesis, low-cost preparation, and universal synthesis strategies). Therefore, it is urgent to develop a universal synthesis strategy to meet the needs of various fields and improve the migration rate of different ions (e.g., Na^+, K^+, Zn^{2+}, Mg^{2+}) in polymer networks by developing universal synthesis methods of crosslinked molecular structures, so as to adapt to different solid-state alkali metal batteries systems (Li/Na/Zn-ion batteries) or supercapacitors (Fig. 12c) [138,143].

5.5. Understanding the electrochemical behaviors of crosslinked SPEs by advanced in-situ characterization techniques

During the whole cycling life of the solid-state batteries, some uncertainties such as continuous monitoring of the dynamic chemistry inside cells and unsustainable multi-interfacial problems remain to be further revealed. The oxidative decomposition/evolution of the electrode/electrolyte interfaces can directly affect the health condition of the battery. Advanced in-situ characterization methods include in-situ TEM, in-situ FT-IR, in-situ NMR and in-situ DMES (Differential electrochemical mass spectrometry), could reveal the evolution of morphology and structure in operating SSPLBs, including electrodes structural transformation, gas production analysis, interfacial evolution, Li-dendrite growth, and oxidative decomposition of SPEs (Fig. 12d) [139, 144–148]. Moreover, operando nondestructive characterization technologies, such as infrared optical fiber, fiber Bragg grating (FBG) sensors and ultrasonic imaging technology, can monitor the parasitic chemical and physical processes inside the battery in real time under working conditions, building a more profound understanding decomposition mechanisms for solid-state electrolytes [10,29,141,149–151]. These advanced characterization techniques will further guide the optimization of electrolyte materials and improvement the electrochemical performance of solid-state batteries.

CRediT authorship contribution statement

Fei Pei: Writing – original draft, Project administration, Investigation, Funding acquisition, Data curation, Conceptualization. **Lin Wu:** Writing – original draft, Investigation, Data curation. **Wenjie Lin:** Writing – original draft, Investigation, Data curation. **Yi Zhang:** Investigation, Data curation. **Qi Kang:** Investigation, Data curation. **Fenghua Zhang:** Investigation, Data curation. **Yuan Shen:** Supervision, Formal analysis. **Qiang Gao:** Investigation, Data curation. **Zhenyu Huang:** Investigation, Data curation. **Yunhui Huang:** Writing – review & editing, Supervision, Project administration, Conceptualization.

Declaration of competing interest

The authors declare that they have no known competing financial interests or personal relationships that could have appeared to influence the work reported in this paper.

Acknowledgements

This work is supported by the National Natural Science Foundation of China (Grant Nos. 52202236 and 52027816), China Postdoctoral Science Foundation (Special Grant, 2024T170300), and China Postdoctoral Science Foundation (General Program 2022M711232).

References

[1] B. Dunn, H. Kamath, J.-M. Tarascon, Electrical energy storage for the grid: a battery of choices, Science 334 (2011) 928–935.
[2] Y. Jie, S. Wang, S. Weng, Y. Liu, M. Yang, C. Tang, X. Li, Z. Zhang, Y. Zhang, Y. Chen, F. Huang, Y. Xu, W. Li, Y. Guo, Z. He, X. Ren, Y. Lu, K. Yang, S. Cao, H. Lin, R. Cao, P. Yan, T. Cheng, X. Wang, S. Jiao, D. Xu, Towards long-life 500 Wh kg^{-1} lithium metal pouch cells via compact ion-pair aggregate electrolytes, Nat. Energy 9 (2024) 987–998.
[3] C.J. Niu, D.Y. Liu, J.A. Lochala, C.S. Anderson, X. Cao, M.E. Gross, W. Xu, J.G. Zhang, M.S. Whittingham, J. Xiao, J. Liu, Balancing interfacial reactions to achieve long cycle life in high-energy lithium metal batteries, Nat. Energy 6 (2021) 723–732.
[4] S. Han, P. Wen, H. Wang, Y. Zhou, Y. Gu, L. Zhang, Y. Shao-Horn, X. Lin, M. Chen, Sequencing polymers to enable solid-state lithium batteries, Nat. Mater. 22 (2023) 1515–1522.
[5] Z. Zhang, Y. Li, R. Xu, W. Zhou, Y. Li, S.T. Oyakhire, Y. Wu, Ji Xu, H. Wang, Z. Yu, D.T. Boyle, W. Huang, Y. Ye, H. Chen, J. Wan, Z. Bao, W. Chiu, Y. Cui, Capturing the swelling of solid-electrolyte interphase in lithium metal batteries, Science 375 (2022) 66–70.
[6] X.Q. Zhang, T. Li, B.Q. Li, R. Zhang, P. Shi, C. Yan, J.Q. Huang, Q. Zhang, A sustainable solid electrolyte interphase for high-energy-density lithium metal batteries under practical conditions, Angew. Chem. Int. Ed. 59 (2020) 3252–3257.
[7] J. Xiang, Y. Wei, Y. Zhong, Y. Yang, H. Cheng, L. Yuan, H. Xu, Y. Huang, Building practical high-voltage cathode materials for lithium-ion batteries, Adv. Mater. 34 (2022) 2200912.
[8] Z. Cao, X. Zheng, Q. Qu, Y. Huang, H. Zheng, Electrolyte design enabling a high-safety and high-performance Si anode with a tailored electrode-electrolyte interphase, Adv. Mater. 33 (2021) 2103178.
[9] J. Qin, F. Pei, R. Wang, L. Wu, Y. Han, P. Xiao, Y. Shen, L. Yuan, Y. Huang, D. Wang, Sulfur vacancies and 1T phase-rich MoS_2 nanosheets as an artificial solid electrolyte interphase for 400 Wh kg^{-1} lithium metal batteries, Adv. Mater. 36 (2024) 2312773.
[10] Y. Zang, P. Peng, F. Pei, R.H. Li, L. Wu, D.Q. Lu, Y. Zhang, K. Huang, Y. Shen, Y.H. Huang, Y.Q. Lan, Conjugated phthalocyanine based framework as artificial SEI for over 400 Wh kg^{-1} lithium metal battery, Natl. Sci. Rev. 12 (2025) nwae443.
[11] Z. Luo, Y. Cao, G. Xu, W. Sun, X. Xiao, H. Liu, S. Wang, Recent advances in robust and ultra-thin Li metal anode, Carbon Neutralization 3 (2024) 647–672.
[12] Z. Wang, J. Zhao, X. Zhang, Z. Rong, Y. Tang, X. Liu, L. Zhu, L. Zhang, J. Huang, Tailoring lithium concentration in alloy anodes for long cycling and high areal capacity in sulfide-based all solid-state batteries, eScience 3 (2023) 100087.
[13] J. Wang, X. Lei, S. Guo, L. Gu, X. Wang, A. Yu, D. Su, Doping strategy in nickel-rich layered oxide cathode for lithium-ion battery, Renewables 1 (2023) 316–340.
[14] A. Hu, W. Chen, F. Li, M. He, D. Chen, Y. Li, J. Zhu, Y. Yan, J. Long, Y. Hu, T. Lei, B. Li, X. Wang, J. Xiong, Nonflammable polyfluorides-anchored quasi-solid electrolytes for ultra-safe anode-free lithium pouch cells without thermal runaway, Adv. Mater. 35 (2023) 2304762.
[15] J. Pan, Y. Zhang, J. Wang, Z. Bai, R. Cao, N. Wang, S. Dou, F. Huang, A quasi-double-layer solid electrolyte with adjustable interphases enabling high-voltage solid-state batteries, Adv. Mater. 34 (2022) 2107183.
[16] Y. Ji, Z. Wang, C. Zhao, Z. Fang, Y. Gong, Q. Jing, Y. Xia, T. Luan, Y. Jiang, J. Liang, X. Li, M. Zhao, X. Zhai, X. Bie, T. Jiang, D. Geng, X. Sun, Diffusion-free all-solid-state batteries enabled by an ionic/electronic dual-conductive anode, Renewables 2 (2024) 194–203.
[17] C. Liao, C. Yu, S. Chen, C. Wei, Z. Wu, S. Chen, Z. Jiang, S. Cheng, J. Xie, Mitigation of the instability of ultrafast Li-ion conductor $Li_{6.6}Si_{0.6}Sb_{0.4}S_5I$ enables high-performance all-solid-state batteries, Renewables 1 (2023) 266–276.
[18] L. Qian, T. Or, Y. Zheng, M. Li, D. Karim, A. Cui, M. Ahmed, H.W. Park, Z. Zhang, Y. Deng, A. Yu, Z. Chen, K. Amine, Critical operation strategies toward high-performance lithium metal batteries, Renewables 1 (2023) 114–141.
[19] D.E. Fenton, J.M. Parker, P.V. Wright, Complexes of alkali metal ions with poly(ethylene oxide), Polymer 14 (1973) 589.
[20] H. Wang, Y. Yang, C. Gao, T. Chen, J. Song, Y. Zuo, Q. Fang, T. Yang, W. Xiao, K. Zhang, X. Wang, D. Xia, An entanglement association polymer electrolyte for Li-metal batteries, Nat. Commun. 15 (2024) 2500.
[21] J. Liu, X. Shen, J. Zhou, M. Wang, C. Niu, T. Qian, C. Yan, Nonflammable and high-voltage-tolerated polymer electrolyte achieving high stability and safety in 4.9 V-class lithium metal battery, ACS Appl. Mater. Interfaces 11 (2019) 45048–45056.
[22] H. Duan, M. Fan, W.P. Chen, J.Y. Li, P.F. Wang, W.P. Wang, J.L. Shi, Y.X. Yin, L.J. Wan, Y.G. Guo, Extended electrochemical window of solid electrolytes via heterogeneous multilayered structure for high-voltage lithium metal batteries, Adv. Mater. 31 (2019) 1807789.
[23] R. Sun, R. Zhu, J. Li, Z. Wang, Y. Zhu, L. Yin, C. Wang, R. Wang, Z. Zhang, The synergy mechanism of $CsSnI_3$ and LiTFSI enhancing the electrochemical performance of PEO-based solid-state batteries, Carbon Neutralization 3 (2024) 597–605.
[24] Q. Kang, Y. Li, Z. Zhuang, D. Wang, C. Zhi, P. Jiang, X. Huang, Dielectric polymer based electrolytes for high-performance all-solid-state lithium metal batteries, J. Energy Chem. 69 (2022) 194–204.
[25] Q. Kang, Z. Zhuang, Y. Liu, Z. Liu, Y. Li, B. Sun, F. Pei, H. Zhu, H. Li, P. Li, Y. Lin, K. Shi, Y. Zhu, J. Chen, C. Shi, Y. Zhao, P. Jiang, Y. Xia, D. Wang, X. Huang, Engineering the structural uniformity of gel polymer electrolytes via pattern-guided alignment for durable, safe solid-state lithium metal batteries, Adv. Mater. 35 (2023) 2303460.
[26] C. Zhang, S. Gamble, D. Ainsworth, A.M. Slawin, Y.G. Andreev, P.G. Bruce, Alkali metal crystalline polymer electrolytes, Nat. Mater. 8 (2009) 580–584.
[27] Q. Zhou, J. Ma, S. Dong, X. Li, G. Cui, Intermolecular chemistry in solid polymer electrolytes for high-energy-density lithium batteries, Adv. Mater. 31 (2019) 1902029.
[28] F. Pei, T.H. An, J. Zang, X.J. Zhao, X.L. Fang, M.S. Zheng, Q.F. Dong, N.F. Zheng, From hollow carbon spheres to N-doped hollow porous carbon bowls: rational design of hollow carbon host for Li-S batteries, Adv. Energy Mater. 6 (2016) 1502539.
[29] F. Pei, L. Wu, Y. Zhang, Y. Liao, Q. Kang, Y. Han, H. Zhang, Y. Shen, H. Xu, Z. Li, Y. Huang, Interfacial self-healing polymer electrolytes for long-cycle solid-state lithium-sulfur batteries, Nat. Commun. 15 (2024) 351.
[30] J. Chen, X. Deng, Y. Gao, Y. Zhao, X. Kong, Q. Rong, J. Xiong, D. Yu, S. Ding, Multiple dynamic bonds-driven integrated cathode/polymer electrolyte for stable all-solid-state lithium metal batteries, Angew. Chem. Int. Ed. 62 (2023) 202307255.
[31] R. Narayan, C. Laberty-Robert, J. Pelta, J.M. Tarascon, R. Dominko, Self-healing: an emerging technology for next-generation smart batteries, Adv. Energy Mater. 12 (2022) 2102652.
[32] Q. Meng, Y. Huang, L. Li, F. Wu, R. Chen, Smart batteries for powering the future, Joule 8 (2024) 344–373.
[33] P. Guo, A. Su, Y. Wei, X. Liu, Y. Li, F. Guo, J. Li, Z. Hu, J. Sun, Healable, highly conductive, flexible, and nonflammable supramolecular ionogel electrolytes for lithium-ion batteries, ACS Appl. Mater. Interfaces 11 (2019) 19413–19420.
[34] X.-Y. Deng, H. Xie, L. Du, C.-J. Fan, C.-Y. Cheng, K.-K. Yang, Y.-Z. Wang, Polyurethane networks based on disulfide bonds: from tunable multi-shape memory effects to simultaneous self-healing, Sci. China Mater. 62 (2018) 437–447.
[35] J. Gui, Z. Huang, J. Lu, L. Wang, Q. Cao, H. Hu, M. Zheng, K. Leng, Y. Liang, High-safety lithium metal batteries enabled by additive of fire-extinguishing microcapsules, Carbon Neutralization 4 (2024) e182, https://doi.org/10.1002/cnl2.182.
[36] Y. Yanagisawa, Y. Nan, K. Okuro, T. Aida, Mechanically robust, readily repairable polymers via tailored noncovalent cross-linking, Science 359 (2018) 72–76.
[37] H. Guo, Y. Han, W. Zhao, J. Yang, L. Zhang, Universally autonomous self-healing elastomer with high stretchability, Nat. Commun. 11 (2020) 2037.
[38] D.G. Mackanic, X. Yan, Q. Zhang, N. Matsuhisa, Z. Yu, Y. Jiang, T. Manika, J. Lopez, H. Yan, K. Liu, X. Chen, Y. Cui, Z. Bao, Decoupling of mechanical properties and ionic conductivity in supramolecular lithium ion conductors, Nat. Commun. 10 (2019) 5384.
[39] G. Beaudoin, A. Lasri, C. Zhao, B. Liberelle, G. De Crescenzo, X.-X. Zhu, Making hydrophilic polymers thermoresponsive: the upper critical solution temperature of copolymers of acrylamide and acrylic acid, Macromolecules 54 (2021) 7963–7969.
[40] S.M. Kim, H. Jeon, S.H. Shin, S.A. Park, J. Jegal, S.Y. Hwang, D.X. Oh, J. Park, Superior toughness and fast self-healing at room temperature engineered by transparent elastomers, Adv. Mater. 30 (2018) 1705145.
[41] Y. Song, Y. Liu, T. Qi, G.L. Li, Towards dynamic but supertough healable polymers through biomimetic hierarchical hydrogen-bonding interactions, Angew. Chem. Int. Ed. 57 (2018) 13838–13842.
[42] L. Wu, F. Pei, D. Cheng, Y. Zhang, H. Cheng, K. Huang, Z. Li, H. Xu, Y. Huang, Flame-retardant polyurethane-based solid-state polymer electrolytes enabled by

covalent bonding for lithium metal batteries, Adv. Funct. Mater. 34 (2024) 2310084.
[43] D.R. Huang, L. Wu, Q. Kang, Z.Y. Shen, Q.S. Huang, W.J. Lin, F. Pei, Y.H. Huang, Amino-modified UiO-66-NH_2 reinforced polyurethane based polymer electrolytes for high-voltage solid-state lithium metal batteries, Nano Res. 17 (2024) 9662–9670.
[44] Y.W. Wen, M. Li, L.F. Fan, M.Z. Rong, M.Q. Zhang, Imparting ultrahigh strength to polymers via a new concept strategy of construction of up to duodecuple hydrogen bonding among macromolecular chains, Adv. Mater. 35 (2024) 2406574.
[45] B. Qin, S. Zhang, P. Sun, B. Tang, Z. Yin, X. Cao, Q. Chen, J.F. Xu, X. Zhang, Tough and multi-recyclable cross-linked supramolecular polyureas via incorporating noncovalent bonds into main-chains, Adv. Mater. 32 (2020) 2000096.
[46] F. Chen, C. Guo, H. Zhou, M.W. Shahzad, T.X. Liu, S. Oleksandr, J. Sun, S. Dai, B.B. Xu, Supramolecular network structured gel polymer electrolyte with high ionic conductivity for lithium metal batteries, Small 18 (2022) 2106352.
[47] A. GhavamiNejad, N. Ashammakhi, X.Y. Wu, A. Khademhosseini, Crosslinking strategies for 3D bioprinting of polymeric hydrogels, Small 16 (2020) 2002931.
[48] J. Liu, Y. Liu, Y. Wang, J. Zhu, J. Yu, Z. Hu, Disulfide bonds and metal-ligand co-crosslinked network with improved mechanical and self-healing properties, Mater. Today Commun. 13 (2017) 282–289.
[49] J. Yoon, D.X. Oh, C. Jo, J. Lee, D.S. Hwang, Improvement of desolvation and resilience of alginate binders for Si-based anodes in a lithium ion battery by calcium-mediated cross-linking, Phys. Chem. Chem. Phys. 16 (2014) 25628–25635.
[50] Y. Chen, Y. Wang, Z. Li, D. Wang, H. Yuan, H. Zhang, Y. Tan, A flame retarded polymer-based composite solid electrolyte improved by natural polysaccharides, Compos. Commun. 26 (2021) 100774.
[51] C. Yang, Q. Wu, W. Xie, X. Zhang, A. Brozena, J. Zheng, M.N. Garaga, B.H. Ko, Y. Mao, S. He, Y. Gao, P. Wang, M. Tyagi, F. Jiao, R. Briber, P. Albertus, C. Wang, S. Greenbaum, Y.Y. Hu, A. Isogai, M. Winter, K. Xu, Y. Qi, L. Hu, Copper-coordinated cellulose ion conductors for solid-state batteries, Nature 598 (2021) 590–596.
[52] L. Zhang, L. Zhang, L. Chai, P. Xue, W. Hao, H. Zheng, A coordinatively cross-linked polymeric network as a functional binder for high-performance silicon submicro-particle anodes in lithium-ion batteries, J. Mater. Chem. A 2 (2014) 19036–19045.
[53] J.Y. Sun, X. Zhao, W.R. Illeperuma, O. Chaudhuri, K.H. Oh, D.J. Mooney, J.J. Vlassak, Z. Suo, Highly stretchable and tough hydrogels, Nature 489 (2012) 133–136.
[54] K. Tang, J. Fu, M. Wu, T. Hua, J. Liu, L. Song, H. Hu, Synergetic chemistry and interface engineering of hydrogel electrolyte to strengthen durability of solid-state Zn-air batteries, Small Methods 6 (2022) 2101276.
[55] X. Song, K. Ma, J. Wang, H. Wang, H. Xie, Z. Zheng, J. Zhang, Three-dimensional metal-organic framework@cellulose skeleton-reinforced composite polymer electrolyte for all-solid-state lithium metal battery, ACS Nano 18 (2024) 12311–12324.
[56] Y. Wei, T.H. Liu, W. Zhou, H. Cheng, X. Liu, J. Kong, Y. Shen, H. Xu, Y. Huang, Enabling all-solid-state li metal batteries operated at 30 °C by molecular regulation of polymer electrolyte, Adv. Energy Mater. 13 (2023) 2203547.
[57] H. Nie, N.S. Schauser, J.L. Self, T. Tabassum, S. Oh, Z. Geng, S.D. Jones, M.S. Zayas, V.G. Reynolds, M.L. Chabinyc, C.J. Hawker, S. Han, C.M. Bates, R.A. Segalman, J. Read de Alaniz, Light-switchable and self-healable polymer electrolytes based on dynamic diarylethene and metal-ion coordination, J. Am. Chem. Soc. 143 (2021) 1562–1569.
[58] X. Wang, S. Zhan, Z. Lu, J. Li, X. Yang, Y. Qiao, Y. Men, J. Sun, Healable, recyclable, and mechanically tough polyurethane elastomers with exceptional damage tolerance, Adv. Mater. 32 (2020) 2005759.
[59] K. Hashimoto, T. Shiwaku, H. Aoki, H. Yokoyama, K. Mayumi, K. Ito, Strain-induced crystallization and phase separation used for fabricating a tough and stiff slide-ring solid polymer electrolyte, Sci. Adv. 9 (2023) eadi8505.
[60] X. Deng, J. Chen, X. Jia, X. Da, Y. Zhao, Y. Gao, Y. Gao, X. Kong, S. Ding, G. Gao, Highly tough slide-crosslinked gel polymer electrolyte for stable lithium metal batteries, Angew. Chem. Int. Ed. 63 (2024) e202410818.
[61] J. Zhao, Z. Zhang, L. Cheng, R. Bai, D. Zhao, Y. Wang, W. Yu, X. Yan, Mechanically interlocked vitrimers, J. Am. Chem. Soc. 144 (2022) 872–882.
[62] L. Chen, X. Sheng, G. Li, F. Huang, Mechanically interlocked polymers based on rotaxanes, Chem. Soc. Rev. 51 (2022) 7046–7065.
[63] Y. Wang, Z. Zhang, H. Zhang, J. Zhao, G. Liu, R. Bai, Y. Liu, W. You, W. Yu, X. Yan, Mechanically interlocked [an]daisy chain networks, Chem 9 (2023) 2206–2221.
[64] J. Seo, G.H. Lee, J. Hur, M.C. Sung, J.H. Seo, D.W. Kim, Mechanically interlocked polymer electrolyte with built-in fast molecular shuttles for all-solid-state lithium batteries, Adv. Energy Mater. 11 (2021) 2102583.
[65] L.D. Sun, Y. Wang, L.C. Kong, S.S. Chen, C. Peng, J.H. Zheng, Y. Li, W. Feng, Designing mesostructured iron (II) fluorides with a stable *in situ* polymer electrolyte interface for high-energy-density lithium-ion batteries, eScience 4 (2024) 100188, https://doi.org/10.1016/j.esci.2023.100188.
[66] S. Choi, T. Kwon, A. Coskun, J.W. Choi, Highly elastic binders integrating polyrotaxanes for silicon microparticle anodes in lithium ion batteries, Science 357 (2017) 279–283.
[67] C.Y. Shi, Q. Zhang, C.Y. Yu, S.J. Rao, S. Yang, H. Tian, D.H. Qu, An ultrastrong and highly stretchable polyurethane elastomer enabled by a zipper-like ring-sliding effect, Adv. Mater. 32 (2020) 2000345.
[68] Z. Shi, Y. Wang, X. Yue, J. Zhao, M. Fang, J. Liu, Y. Chen, Y. Dong, X. Yan, Z. Liang, Mechanically interlocked interphase with energy dissipation and fast Li-ion transport for high-capacity lithium metal batteries, Adv. Mater. 36 (2024) 2401711.
[69] P. Ding, L. Wu, Z. Lin, C. Lou, M. Tang, X. Guo, H. Guo, Y. Wang, H. Yu, Molecular self-assembled ether-based polyrotaxane solid electrolyte for lithium metal batteries, J. Am. Chem. Soc. 145 (2023) 1548–1556.
[70] S. Qi, M. Li, Y. Gao, W. Zhang, S. Liu, J. Zhao, L. Du, Enabling scalable polymer electrolyte with dual-reinforced stable interface for 4.5 V lithium-metal batteries, Adv. Mater. 35 (2023) 2304951.
[71] S.J. Yang, H. Yuan, N. Yao, J.K. Hu, X.L. Wang, R. Wen, J. Liu, J.Q. Huang, Intrinsically safe lithium metal batteries enabled by thermo-electrochemical compatible in situ polymerized solid-state electrolytes, Adv. Mater. 36 (2024) 2405086.
[72] J. Li, T. Zhang, X. Hui, R. Zhu, Q. Sun, X. Li, L. Yin, Competitive Li^+ coordination in ionogel electrolytes for enhanced Li-ion transport kinetics, Adv. Sci. 10 (2023) 2300226.
[73] N. Xu, Y. Zhao, M. Ni, J. Zhu, X. Song, X. Bi, J. Zhang, H. Zhang, Y. Ma, C. Li, Y. Chen, In-situ cross-linked F- and P-containing solid polymer electrolyte for long-cycling and high-safety lithium metal batteries with various cathode materials, Angew. Chem. Int. Ed. 63 (2024) e202404400.
[74] Y. Zhang, Z. Wang, Y. Pan, H. Yu, Z. Li, C. Li, S. Wang, Y. Ma, X. Shi, H. Zhang, D. Song, L. Zhang, Tailoring a multi-system adaptable gel polymer electrolyte for the realization of carbonate ester and ether-based Li-SPAN batteries, Energy Environ. Sci. 17 (2024) 2576–2587.
[75] M. Wang, H. Zhang, Y. Li, R. Liu, H. Yang, A three-dimensional co-continuous network structure polymer electrolyte with efficient ion transport channels enabling ultralong-life all solid-state lithium metal batteries, J. Energy Chem. 94 (2024) 635–645.
[76] L. Nie, S. Chen, M. Zhang, T. Gao, Y. Zhang, R. Wei, Y. Zhang, W. Liu, An in-situ polymerized interphase engineering for high-voltage all-solid-state lithium-metal batteries, Nano Res. 17 (2023) 2687–2692.
[77] L. Wang, S.G. Xu, Z. Wang, E.E. Yang, W.Y. Jiang, S.H. Zhang, X.G. Jian, F.Y. Hu, A nano fiber-gel composite electrolyte with high Li^+ transference number for application in quasi-solid batteries, eScience 3 (2023) 100090, https://doi.org/10.1016/j.esci.2022.100090.
[78] M.J. Lee, J. Han, K. Lee, Y.J. Lee, B.G. Kim, K.N. Jung, B.J. Kim, S.W. Lee, Elastomeric electrolytes for high-energy solid-state lithium batteries, Nature 601 (2022) 217–222.
[79] L. Tang, B. Chen, Z. Zhang, C. Ma, J. Chen, Y. Huang, F. Zhang, Q. Dong, G. Xue, D. Chen, C. Hu, S. Li, Z. Liu, Y. Shen, Q. Chen, L. Chen, Polyfluorinated crosslinker-based solid polymer electrolytes for long-cycling 4.5 V lithium metal batteries, Nat. Commun. 14 (2023) 2301.
[80] J. Zhu, R. Zhao, J. Zhang, X. Song, J. Liu, N. Xu, H. Zhang, X. Wan, X. Ji, Y. Ma, C. Li, Y. Chen, Long-cycling and high-voltage solid state lithium metal batteries enabled by fluorinated and crosslinked polyether electrolytes, Angew. Chem. Int. Ed. 63 (2024) e202400303.
[81] J. Zhu, J. Zhang, R. Zhao, Y. Zhao, J. Liu, N. Xu, X. Wan, C. Li, Y. Ma, H. Zhang, Y. Chen, In situ 3D crosslinked gel polymer electrolyte for ultra-long cycling, high-voltage, and high-safety lithium metal batteries, Energy Storage Mater. 57 (2023) 92–101.
[82] S. Wen, C. Luo, Q. Wang, Z. Wei, Y. Zeng, Y. Jiang, G. Zhang, H. Xu, J. Wang, C. Wang, J. Chang, Y. Deng, Integrated design of ultrathin crosslinked network polymer electrolytes for flexible and stable all-solid-state lithium batteries, Energy Storage Mater. 47 (2022) 453–461.
[83] J. Liang, R. Tao, J. Tu, C. Guo, K. Du, R. Guo, W. Zhang, X. Liu, P. Guo, D. Wang, S. Dai, X.-G. Sun, Design of a multi-functional gel polymer electrolyte with a 3D compact stacked polymer micro-sphere matrix for high-performance lithium metal batteries, J. Mater. Chem. A 10 (2022) 12563–12574.
[84] W. Tang, T. Zhou, Y. Duan, M. Zhou, Z. Li, R. Liu, Nonflammable in situ PDOL-based gel polymer electrolyte for high-energy-density and high safety lithium metal batteries, Carbon Neutralization 3 (2024) 386–395.
[85] F.Q. Liu, W.P. Wang, Y.X. Yin, S.F. Zhang, J.L. Shi, L. Wang, X.D. Zhang, Y. Zheng, J.J. Zhou, L. Li, Y.G. Guo, Upgrading traditional liquid electrolyte via in situ gelation for future lithium metal batteries, Sci. Adv. 4 (2018) eaat5383.
[86] S. Choudhury, R. Mangal, A. Agrawal, L.A. Archer, A highly reversible room-temperature lithium metal battery based on crosslinked hairy nanoparticles, Nat. Commun. 6 (2015) 10101.
[87] X. Cai, J. Ding, Z. Chi, W. Wang, D. Wang, G. Wang, Rearrangement of ion transport path on nano-cross-linker for all-solid-state electrolyte with high room temperature ionic conductivity, ACS Nano 15 (2021) 20489–20503.
[88] D. Chen, T. Zhu, M. Zhu, S. Yuan, P. Kang, W. Cui, J. Lan, X. Yang, G. Sui, In-situ constructing "ceramer" electrolytes with robust-flexible interfaces enabling long-cycling lithium metal batteries, Energy Storage Mater. 53 (2022) 937–945.
[89] K. Mu, W. Dong, W. Xu, Z. Song, R. Wang, L. Wu, H. Li, Q. Liu, C. Zhu, J. Xu, L. Tian, In situ hybrid crosslinking polymerization of nanoparticles for composite polymer electrolytes to achieve highly-stable solid lithium-metal batteries, Adv. Funct. Mater. 34 (2024) 2405969.
[90] W. Liu, S.W. Lee, D. Lin, F. Shi, S. Wang, A.D. Sendek, Y. Cui, Enhancing ionic conductivity in composite polymer electrolytes with well-aligned ceramic nanowires, Nat. Energy 2 (2017) 17035.
[91] F. Pei, S.Q. Dai, B.F. Guo, H. Xie, C.W. Zhao, J.Q. Cui, X.L. Fang, C.M. Chen, N.F. Zheng, Titanium-oxo cluster reinforced gel polymer electrolyte enabling lithium-sulfur batteries with high gravimetric energy densities, Energy Environ. Sci. 14 (2021) 975–985.
[92] L.Z. Fan, H.C. He, C.W. Nan, Tailoring inorganic-polymer composites for the mass production of solid-state batteries, Nat. Rev. Mater. 6 (2021) 1003–1019.
[93] S. Gowneni, K. Ramanjaneyulu, P. Basak, Polymer-nanocomposite brush-like architectures as an all-solid electrolyte matrix, ACS Nano 8 (2014) 11409–11424.

[94] S. Tang, Q. Lan, L. Xu, J.Y. Liang, P. Lou, C. Liu, L.Q. Mai, Y.C. Cao, S.J. Cheng, A novel cross-linked nanocomposite solid-state electrolyte with super flexibility and performance for lithium metal battery, Nano Energy 71 (2020) 104600.

[95] Y. Ou, T. Zhao, Y. Zhang, G. Zhao, L. Dong, Stretchable solvent-free ionic conductor with self-wrinkling microstructures for ultrasensitive strain sensor, Mater. Horiz. 9 (2022) 1679–1689.

[96] Q. Zhou, J. Jian, C. Kang, W. Tang, W. Zhao, Y. Wang, J. Yan, C. Fu, H. Huo, P. Zuo, Solvation structure reorganization and interface regulation of poly (glycidyl POSS)-based electrolyte for quasi-solid-state lithium-ion batteries, Nano Energy 117 (2023) 108892.

[97] Y. Li, C. Zheng, S.T. Wang, Y.J. Liu, W.H. Fang, J. Zhang, Record aluminum molecular rings for optical limiting and nonlinear optics, Angew. Chem. Int. Ed. 61 (2022) 202116563.

[98] Q. Pan, D.M. Smith, H. Qi, S. Wang, C.Y. Li, Hybrid electrolytes with controlled network structures for lithium metal batteries, Adv. Mater. 27 (2015) 5995–6001.

[99] K. Mu, D. Wang, W. Dong, Q. Liu, Z. Song, W. Xu, P. Yao, Y.a. Chen, B. Yang, C. Li, L. Tian, C. Zhu, J. Xu, Hybrid crosslinked solid polymer electrolyte via in-situ solidification enables high-performance solid-state lithium metal batteries, Adv. Mater. 35 (2023) 2304686.

[100] Y. Zheng, C. Wang, R. Zhang, S. Dai, H. Xie, J. Cui, X. Fang, Crosslinked polymer electrolyte constructed by metal-oxo clusters for solid lithium metal batteries, Energy Storage Mater. 57 (2023) 540–548.

[101] Y. Zhang, Y. Liu, W. Bao, X. Zhang, P. Yan, X. Yao, M.Z. Chen, T.Y. Xie, L. Cao, X. Cai, H. Li, Y. Deng, L. Zhao, M.H. Zeng, S. Jiang, Y. Zhao, J. Xie, Monolithic titanium alkoxide networks for lithium-ion conductive all-solid-state electrolytes, Nano Lett. 23 (2023) 4066–4073.

[102] B.W. Liu, H.B. Zhao, Y.Z. Wang, Advanced flame-retardant methods for polymeric materials, Adv. Mater. 34 (2021) 2107905.

[103] X. Wang, Y. Li, Y. Qian, H. Qi, J. Li, J. Sun, Mechanically robust atomic oxygen-resistant coatings capable of autonomously healing damage in low earth orbit space environment, Adv. Mater. 30 (2018) 1803854.

[104] J. Zhang, C. Ma, J. Liu, L. Chen, A. Pan, W. Wei, Solid polymer electrolyte membranes based on organic/inorganic nanocomposites with star-shaped structure for high performance lithium ion battery, J. Membr. Sci. 509 (2016) 138–148.

[105] C. Zhao, Y.Z. Han, S. Dai, X. Chen, J. Yan, W. Zhang, H. Su, S. Lin, Z. Tang, B.K. Teo, N. Zheng, Microporous cyclic titanium-oxo clusters with labile surface ligands, Angew. Chem. Int. Ed. 56 (2017) 16252–16256.

[106] P. Zhai, R. Shao, C. Zeng, S. Qu, F. Pei, Y. Li, W. Yang, Robust ion-rectifying polymer electrolyte membrane for high-rate solid-state lithium metal batteries, Chem. Eng. J. 473 (2023) 144840.

[107] Wenda Bao, Yue Zhang, Lei Cao, Yilan Jiang, Hui Zhang, Nian Zhang, Ying Liu, Pu Yan, Xingzhi Wang, Yixiao Liu, Haoyuan Li, Yingbo Zhao, J. Xie, An H_2O-initiated crosslinking strategy for ultrafine-nanoclusters-reinforced high-toughness polymer-in-plasticizer solid electrolyte, Adv. Mater. 35 (2023) 2304712.

[108] H. Wang, Q. Wang, X. Cao, Y. He, K. Wu, J. Yang, H. Zhou, W. Liu, X. Sun, Thiol-branched solid polymer electrolyte featuring high strength, toughness, and lithium ionic conductivity for lithium-metal batteries, Adv. Mater. 32 (2020) 2001259.

[109] J. Zhou, X. Wang, J. Fu, L. Chen, X. Wei, R. Jia, L. Shi, A 3D cross-linked metal-organic framework (MOF)-derived polymer electrolyte for dendrite-free solid-state lithium-ion batteries, Small 20 (2023) 2309317.

[110] Z. Wang, S. Wang, A. Wang, X. Liu, J. Chen, Q. Zeng, L. Zhang, W. Liu, L. Zhang, Covalently linked metal–organic framework (MOF)-polymer all-solid-state electrolyte membranes for room temperature high performance lithium batteries, J. Mater. Chem. A 6 (2018) 17227–17234.

[111] X. Lu, H. Wu, D. Kong, X. Li, L. Shen, Y. Lu, Facilitating lithium-ion conduction in gel polymer electrolyte by metal-organic frameworks, ACS Mater. Lett. 2 (2020) 1435–1441.

[112] M. Tian, F. Pei, M.S. Yao, Z.H. Fu, L.L. Lin, G.D. Wu, G. Xu, H. Kitagawa, X.L. Fang, Ultrathin MOF nanosheet assembled highly oriented microporous membrane as an interlayer for lithium-sulfur batteries, Energy Storage Mater. 21 (2019) 14–21.

[113] Y. Zang, F. Pei, J.H. Huang, Z.H. Fu, G. Xu, X.L. Fang, Large-area preparation of crack-free crystalline microporous conductive membrane to upgrade high energy lithium-sulfur batteries, Adv. Energy Mater. 8 (2018) 1802052.

[114] Q. Zeng, J. Wang, X. Li, Y. Ouyang, W. He, D. Li, S. Guo, Y. Xiao, H. Deng, W. Gong, Q. Zhang, S. Huang, Cross-linked chains of metal-organic framework afford continuous ion transport in solid batteries, ACS Energy Lett. 6 (2021) 2434–2441.

[115] J. Lopez, Y. Sun, D.G. Mackanic, M. Lee, A.M. Foudeh, M.S. Song, Y. Cui, Z. Bao, A dual-crosslinking design for resilient lithium-ion conductors, Adv. Mater. 30 (2018) 1804142.

[116] Q. Lu, Y.B. He, Q. Yu, B. Li, Y.V. Kaneti, Y. Yao, F. Kang, Q.H. Yang, Dendrite-free, high-rate, long-life lithium metal batteries with a 3D cross-linked network polymer electrolyte, Adv. Mater. 29 (2017) 1604460.

[117] R. Khurana, J.L. Schaefer, L.A. Archer, G.W. Coates, Suppression of lithium dendrite growth using cross-linked polyethylene/poly(ethylene oxide) electrolytes: a new approach for practical lithium-metal polymer batteries, J. Am. Chem. Soc. 136 (2014) 7395–7402.

[118] K. Tang, Q. Bai, P. Xu, R. Liu, S. Xue, S. Liu, Y. Zhu, A thiol branched 3D network quasi solid-state polymer electrolyte reinforced by covalent organic frameworks for lithium metal batteries, Small Methods 8 (2024) 2301810.

[119] H. Wang, X. Li, Q. Zeng, Z. Li, Y. Liu, J. Guan, Y. Jiang, L. Chen, Y. Cao, R. Li, A. Wang, Z.-X. Wang, L. Zhang, A novel hyperbranched polyurethane solid electrolyte for room temperature ultra-long cycling lithium-ion batteries, Energy Storage Mater. 66 (2024) 103188.

[120] J. Sheng, Q. Zhang, C. Sun, J. Wang, X. Zhong, B. Chen, C. Li, R. Gao, Z. Han, G. Zhou, Crosslinked nanofiber-reinforced solid-state electrolytes with polysulfide fixation effect towards high safety flexible lithium-sulfur batteries, Adv. Funct. Mater. 32 (2022) 2203272.

[121] W. Chen, T. Qian, J. Xiong, N. Xu, X. Liu, J. Liu, J. Zhou, X. Shen, T. Yang, Y. Chen, C. Yan, A new type of multifunctional polar binder: toward practical application of high energy lithium sulfur batteries, Adv. Mater. 29 (2017) 1605160.

[122] Z. Fang, Y. Luo, H. Liu, Z. Hong, H. Wu, F. Zhao, P. Liu, Q. Li, S. Fan, W. Duan, J. Wang, Boosting the oxidative potential of polyethylene glycol-based polymer electrolyte to 4.36 V by spatially restricting hydroxyl groups for high-voltage flexible lithium-ion battery applications, Adv. Sci. 8 (2021) 2100736.

[123] Z.X. Xu, J. Yang, T. Zhang, Y.N. Nuli, J.L. Wang, S.I. Hirano, Silicon microparticle anodes with self-healing multiple network binder, Joule 2 (2018) 950–961.

[124] F. Pei, L.L. Lin, A. Fu, S.G. Mo, D.H. Ou, X.L. Fang, N.F. Zheng, A two-dimensional porous carbon-modified separator for high-energy-density Li-S batteries, Joule 2 (2018) 323–336.

[125] L.L. Lin, F. Pei, J. Peng, A. Fu, J.Q. Cui, X.L. Fang, N.F. Zheng, Fiber network composed of interconnected yolk-shell carbon nanospheres for high-performance lithium-sulfur batteries, Nano Energy 54 (2018) 50–58.

[126] F. Pei, L.L. Lin, D.H. Ou, Z.M. Zheng, S.G. Mo, X.L. Fang, N.F. Zheng, Self-supporting sulfur cathodes enabled by two-dimensional carbon yolk-shell nanosheets for high-energy-density lithium-sulfur batteries, Nat. Commun. 8 (2017) 482.

[127] G. Wu, Y. Gao, Z. Weng, Z. Zheng, W. Fan, A. Pan, N. Zhang, X. Liu, R. Ma, G. Chen, Binder-induced inorganic-rich solid electrolyte interphase and physicochemical dual cross-linked network for high-performance SiOx anode, Carbon Neutralization 3 (2024) 857–872.

[128] T. Kwon, Y.K. Jeong, E. Deniz, S.Y. AlQaradawi, J.W. Choi, A. Coskun, Dynamic cross-linking of polymeric binders based on host-guest interactions for silicon anodes in lithium ion batteries, ACS Nano 9 (2015) 11317–11324.

[129] F. Yu, H. Zhang, L. Zhao, Z. Sun, Y. Li, Y. Mo, Y. Chen, A flexible Cellulose/Methylcellulose gel polymer electrolyte endowing superior Li^+ conducting property for lithium ion battery, Carbohydr. Polym. 246 (2020) 116622.

[130] Y. Lin, J. Li, K. Liu, Y. Liu, J. Liu, X. Wang, Unique starch polymer electrolyte for high capacity all-solid-state lithium sulfur battery, Green Chem. 18 (2016) 3796–3803.

[131] W. Gu, F. Li, T. Liu, S. Gong, Q. Gao, J. Li, Z. Fang, Recyclable, self-healing solid polymer electrolytes by soy protein-based dynamic network, Adv. Sci. 9 (2022) 2103623.

[132] O. Sheng, C. Jin, T. Yang, Z. Ju, J. Luo, X. Tao, Designing biomass-integrated solid polymer electrolytes for safe and energy-dense lithium metal batteries, Energy Environ. Sci. 16 (2023) 2804–2824.

[133] J. Li, Z. Hu, S. Zhang, H. Zhang, S. Guo, G. Zhong, Y. Qiao, Z. Peng, Y. Li, S. Chen, G. Chen, A.-M. Cao, Molecular engineering of renewable cellulose biopolymers for solid-state battery electrolytes, Nat. Sustain. 7 (2024) 1481–1491.

[134] Y. Su, X. Wang, M. Zhang, H. Guo, H. Sun, G. Huang, D. Liu, G. Zhu, Porous cyclodextrin polymer enables dendrite-free and ultra-long life solid-state Zn-I_2 batteries, Angew. Chem. Int. Ed. 62 (2023) e202308182.

[135] X. Fan, R. Zhang, S. Sui, X. Liu, J. Liu, C. Shi, N. Zhao, C. Zhong, W. Hu, Starch-based superabsorbent hydrogel with high electrolyte retention capability and synergistic interface engineering for long-lifespan flexible zinc-air batteries, Angew. Chem. Int. Ed. 62 (2023) 202302640.

[136] D. Wang, H. Xie, Q. Liu, K. Mu, Z. Song, W. Xu, L. Tian, C. Zhu, J. Xu, Low-cost, high-strength cellulose-based quasi-solid polymer electrolyte for solid-state lithium-metal batteries, Angew. Chem. Int. Ed. 62 (2023) e202302767.

[137] Q. Zhao, X. Liu, S. Stalin, K. Khan, L.A. Archer, Solid-state polymer electrolytes with in-built fast interfacial transport for secondary lithium batteries, Nat. Energy 4 (2019) 365–373.

[138] W. Zhang, J. Zhang, X. Liu, H. Li, Y. Guo, C. Geng, Y. Tao, Q.H. Yang, In-situ polymerized gel polymer electrolytes with high room-temperature ionic conductivity and regulated Na^+ solvation structure for sodium metal batteries, Adv. Funct. Mater. 32 (2022) 2201205.

[139] S. Zhou, J. Shi, S. Liu, G. Li, F. Pei, Y. Chen, J. Deng, Q. Zheng, J. Li, C. Zhao, I. Hwang, C.J. Sun, Y. Liu, Y. Deng, L. Huang, Y. Qiao, G.L. Xu, J.F. Chen, K. Amine, S.G. Sun, H.G. Liao, Visualizing interfacial collective reaction behaviour of Li-S batteries, Nature 621 (2023) 75–81.

[140] Z. Deng, Z. Huang, Y. Shen, Y. Huang, H. Ding, A. Luscombe, M. Johnson, J.E. Harlow, R. Gauthier, J.R. Dahn, Ultrasonic scanning to observe wetting and "unwetting" in Li-ion pouch cells, Joule 4 (2020) 2017–2029.

[141] J. Huang, L. Albero Blanquer, J. Bonefacino, E.R. Logan, D. Alves Dalla Corte, C. Delacourt, B.M. Gallant, S.T. Boles, J.R. Dahn, H.-Y. Tam, J.-M. Tarascon, Operando decoding of chemical and thermal events in commercial Na(Li)-ion cells via optical sensors, Nat. Energy 5 (2020) 674–683.

[142] K. He, S.H. Cheng, J. Hu, Y. Zhang, H. Yang, Y. Liu, W. Liao, D. Chen, C. Liao, X. Cheng, Z. Lu, J. He, J. Tang, R.K.Y. Li, C. Liu, In-situ intermolecular interaction in composite polymer electrolyte for ultralong life quasi-solid-state lithium metal batteries, Angew. Chem. Int. Ed. 60 (2021) 12116–12123.

[143] H. Zhang, X. Gan, Y. Yan, J. Zhou, A sustainable dual cross-linked cellulose hydrogel electrolyte for high-performance zinc-metal batteries, Nano-Micro Lett. 16 (2024) 106.

[144] F. Pei, A. Fu, W. Ye, J. Peng, X. Fang, M.S. Wang, N. Zheng, Robust lithium metal anodes realized by lithiophilic 3D porous current collectors for constructing high-energy lithium-sulfur batteries, ACS Nano 13 (2019) 8337–8346.

[145] J. Wan, H.-J. Yan, R. Wen, L.-J. Wan, In situ visualization of electrochemical processes in solid-state lithium batteries, ACS Energy Lett. 7 (2022) 2988–3002.

[146] H. Gao, X. Ai, H. Wang, W. Li, P. Wei, Y. Cheng, S. Gui, H. Yang, Y. Yang, M.S. Wang, Visualizing the failure of solid electrolyte under GPa-level interface stress induced by lithium eruption, Nat. Commun. 13 (2022) 5050.
[147] W.B. Ye, F. Pei, X.N. Lan, Y. Cheng, X.L. Fang, Q.B. Zhang, N.F. Zheng, D.L. Peng, M.S. Wang, Stable nano-encapsulation of lithium through seed-free selective deposition for high-performance Li battery anodes, Adv. Energy Mater. 10 (2020) 1902956.
[148] T. Yi, E. Zhao, Y. He, T. Liang, H. Wang, Quantification and visualization of spatial distribution of dendrites in solid polymer electrolytes, eScience 4 (2024) 100182.
[149] C. Gervillié-Mouravieff, C. Boussard-Plédel, J. Huang, C. Leau, L.A. Blanquer, M.B. Yahia, M.L. Doublet, S.T. Boles, X.H. Zhang, J.L. Adam, J.M. Tarascon, Unlocking cell chemistry evolution with operando fibre optic infrared spectroscopy in commercial Na(Li)-ion batteries, Nat. Energy 7 (2022) 1157–1169.
[150] J. Huang, S.T. Boles, J.-M. Tarascon, Sensing as the key to battery lifetime and sustainability, Nat. Sustain. 5 (2022) 194–204.
[151] Y. Zhang, S. Hao, F. Pei, X. Xiao, C. Lu, X. Lin, Z. Li, H. Ji, Y. Shen, L. Yuan, Z. Li, Y. Huang, Operando chemo-mechanical evolution in $LiNi_{0.8}Co_{0.1}Mn_{0.1}O_2$ cathodes, Natl. Sci. Rev. 11 (2024) nwae254.